

Supporting Information

---

***A new C,N-cyclometalated osmium(II) arene anticancer scaffold  
with a handle for functionalization and antioxidative properties***

Enrique Ortega,<sup>a</sup> Jyoti G. Yellol,<sup>a</sup> Matthias Rothemund,<sup>b</sup> Francisco J. Ballester,<sup>a</sup>  
Venancio Rodríguez,<sup>a</sup> Gorakh Yellol,<sup>a</sup> Christoph Janiak,<sup>c</sup> Rainer Schobert,<sup>b</sup> José Ruiz.<sup>a</sup>

*<sup>a</sup>Departamento de Química Inorgánica and Regional Campus of International  
Excellence “Campus Mare Nostrum”, Universidad de Murcia, and Biomedical  
Research Institute of Murcia (IMIB-Arrixaca), E-30071 Murcia, Spain Tel: + 34  
868887455, Email: jruiz@um.es.*

*<sup>b</sup>Organic Chemistry Laboratory, University Bayreuth, Bayreuth, Universitaetsstrasse  
30, D-95440, Germany*

*<sup>c</sup>Institut für Anorganische Chemie und Strukturchemie, Heinrich-Heine-Universität  
Düsseldorf, Universitätsstrasse 1, D-40225 Düsseldorf, Germany*

**Table of Contents**

Starting materials and reagents	2
Instrumentation	3
Synthesis of osmium compounds	3
General procedure for synthesis of osmium compounds <b>1-6</b> .	3
Compound <b>1</b>	4
Compound <b>2</b>	4
Compound <b>3</b>	5
Compound <b>4</b>	6
Compound <b>5</b>	6
Compound <b>6</b>	7
NMR spectra of compounds <b>1-6</b>	8
Hydrolysis Studies	15

HPLC-MS stability study	16
Reaction with NAD <sup>+</sup>	17
Cell lines and culture media	18
Cytotoxicity Assays	19
Apoptotic induction	20
Mitochondrial polarization assay.	21
Intracellular reactive oxygen species (ROS) determination.	24
Cell cycle distribution perturbation	25
Metal accumulation	26
Tubulin polymerization inhibition assay	27
X-ray Crystallographic Analysis	28
Supramolecular packing analysis for compound <b>1</b>	40
References	46

### **Starting materials and reagents**

All synthetic manipulations were carried out under an atmosphere of dry, oxygen-free nitrogen using standard Schlenk techniques. Solvents were dried by the usual methods. Substituted benzaldehydes, trifluoroacetic acid, magnesium sulfate, sodium sulfate, sodium acetate, CDDP [purity  $\geq$  99.9% based on elemental and inductively coupled plasma mass spectroscopy (ICP-MS) trace analysis] and dimethyl sulfoxide (DMSO) were obtained from Sigma-Aldrich (Madrid, Spain) and osmium(III) chloride hydrate from Johnson Matthey. Deuterated solvents were obtained from Euriso-top.  $[(\eta^6\text{-}p\text{-cymene})\text{OsCl}_2]_2$  was prepared as previously reported.<sup>1</sup> Benzimidazole pro-ligands were prepared as reported elsewhere.<sup>2,3</sup> The purity of all biologically evaluated molecules, based on elemental analysis, is >95%.

Stock solutions for cellular studies were prepared by dissolving the osmium compounds in DMSO to a final concentration of 20 mM and serially diluted prior to

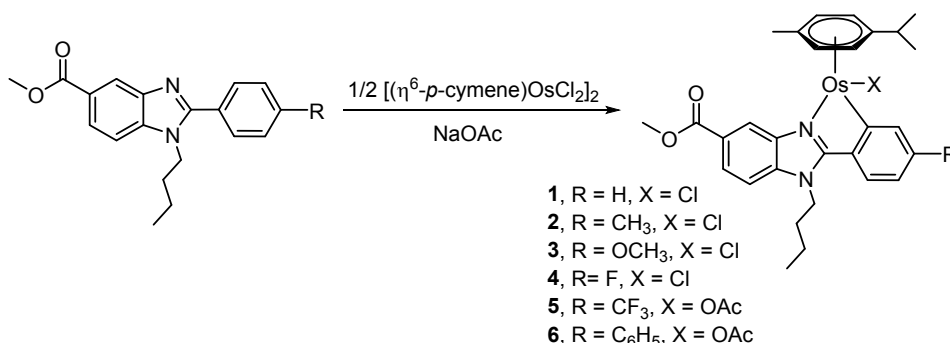
testing in DMSO. To avoid DMSO toxicity, the final DMSO concentration in culture medium didn't exceed 0.4 % (v/v). CDDP stock solution was prepared by dissolving CDDP in ultrapure water (Milli-Q®, Merck Millipore) to a final concentration of 20 mM

## Instrumentation

The C, H, and N analyses were performed with a Carlo Erba model EA 1108 microanalyzer. The  $^1\text{H}$  and  $^{13}\text{C}$  spectra were recorded on a Bruker AC 200E, Bruker AC 300E, Bruker AV 400, or Bruker AV 600 NMR spectrometer in 5 mm NMR tubes at 298 K. Chemical shifts are cited relative to  $\text{SiMe}_4$  ( $^1\text{H}$  and  $^{13}\text{C}$ , external) and  $\text{CFCl}_3$  ( $^{19}\text{F}$ ). ESI mass (positive mode) analyses were performed on a HPLC/MS TOF 6220. The isotopic distribution of the heaviest set of peaks matched very closely that calculated for the formulation of the complex cation in every case. The FT-IR spectra were recorded on a Perkin-Elmer 1430 spectrophotometer using Nujol mulls between polyethylene sheets. UV/vis spectroscopy was carried out on a Perkin-Elmer Lambda 750 S spectrometer with operating software.

## Synthesis of osmium compounds

### General procedure for synthesis of osmium compounds 1-6.

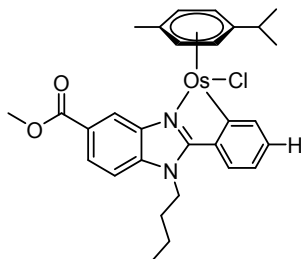


### Scheme S1. Synthesis of the osmium(II) compounds.

The respective benzimidazole core ligand (R = H, CH<sub>3</sub>, OCH<sub>3</sub>, F, CF<sub>3</sub>, C<sub>6</sub>H<sub>5</sub>) (1.0 mmol) was dissolved in freshly distilled dichloromethane in dry round bottom flask equipped with stirrer and nitrogen atmosphere. Sodium acetate (2.2 mmol) was added in it at room temperature with constant stirring followed by addition of  $[(\eta^6\text{-}p\text{-cymene})\text{OsCl}_2]_2$  (0.5 mmol). The reaction mixture was stirred at room temperature for 24 h and progress of reaction was monitored by TLC. After complete conversion, reaction mixture was filtered through celite bed (for removal of NaCl). Dichloromethane was removed under reduced pressure and product was precipitated in diethyl ether (10 mL). The solid was separated by filtration and dried to obtain the respective osmium compound

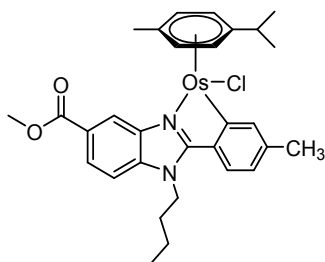
(1-6) in moderate yields. Crystals suitable for X-ray diffraction were obtained for complexes **1** and **6** in CH<sub>2</sub>Cl<sub>2</sub>/toluene/hexane mixture (2:1:3).

### Compound 1



Yellow solid; Yield (66%); <sup>1</sup>H NMR (300 MHz, CDCl<sub>3</sub>) δ 8.47 (d, *J* = 1.2 Hz, 1H), 8.22 (dd, *J* = 7.5, 0.9 Hz, 1H), 8.06 (dd, *J* = 8.4, 1.5 Hz, 1H), 7.72 (dd, *J* = 7.8, 0.9 Hz, 1H), 7.40 (d, *J* = 8.4 Hz, 1H), 7.17 (dt, *J* = 7.2, 1.2 Hz, 1H), 7.08 (t, *J* = 7.5, 1.2 Hz, 1H), 5.92 (d, *J* = 5.4 Hz, 1H), 5.76 (d, *J* = 5.3 Hz, 1H), 5.63 (d, *J* = 5.4 Hz, 1H), 5.36 (d, *J* = 5.3 Hz, 1H), 4.50 (m, 2H), 4.02 (s, 3H), 2.23 (m, 4H), 1.95 (m, 2H), 1.46 (m, 2H), 0.97 (t, *J* = 7.5 Hz, 3H), 0.92 (d, *J* = 6.9 Hz, 3H), 0.73 (d, *J* = 6.9 Hz, 3H); <sup>13</sup>C NMR (50 MHz, CDCl<sub>3</sub>) δ 169.7, 167.1, 163.2, 140.7, 140.4, 138.9, 132.9, 130.3, 125.3, 124.6, 124.2, 122.5, 119.4, 109.7, 95.1, 89.7, 79.9, 78.8, 72.6, 70.6, 52.3, 44.8, 31.7, 31.2, 22.9, 21.9, 20.1, 18.8, 13.7; IR (Nujol, cm<sup>-1</sup>): ν(Os-Cl) 286; ESI-MS (pos ion mode, CH<sub>2</sub>Cl<sub>2</sub>): *m/z* = 633.2222 ([M-Cl])<sup>+</sup>; Anal. Calcd for C<sub>29</sub>H<sub>33</sub>ClN<sub>2</sub>O<sub>2</sub>Os (667.28): C, 52.20; H, 4.99; N, 4.20; Found: C, 52.03; H, 5.17; N, 4.10 (%).

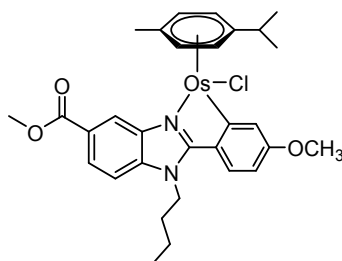
### Compound 2



Yellow solid. Yield (49%). <sup>1</sup>H NMR (600 MHz, CDCl<sub>3</sub>) δ 8.43 (s, 1H), 8.05 (dd, *J* = 8.5, 1.0 Hz, 1H), 8.03 (s, 1H), 7.61 (d, *J* = 7.9 Hz, 1H), 7.39 (d, *J* = 8.5 Hz, 1H), 6.90 (dd, *J* = 8.5, 1.0 Hz, 1H), 5.90 (d, *J* = 5.4 Hz, 1H), 5.74 (d, *J* = 5.2 Hz, 1H), 5.64 (d, *J* = 5.4 Hz, 1H), 5.34 (d, *J* = 5.2 Hz, 1H), 4.62 (m, 1H), 4.45 (m, 1H), 4.00 (s, 3H), 2.17 (m, 1H), 2.43 (s, 3H), 2.25 (s, 3H), 1.94 (m, 2H), 1.44 (m, 2H), 0.98 (t, *J* = 7.3 Hz, 3H), 0.91 (d, *J*

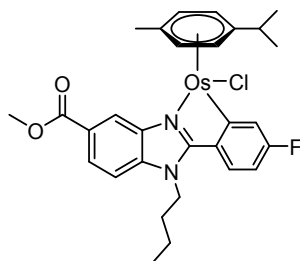
= 6.8 Hz, 3H), 0.73 (d,  $J = 6.8$  Hz, 3H);  $^{13}\text{C}$  NMR (151 MHz,  $\text{CDCl}_3$ )  $\delta$  169.82, 167.18, 163.35, 141.29, 140.54, 140.32, 139.00, 130.31, 125.19, 124.48, 123.98, 123.81, 119.24, 109.52, 95.08, 89.39, 79.82, 78.76, 72.78, 70.38, 52.26, 44.73, 31.68, 31.25, 22.95, 22.01, 21.73, 20.11, 18.78, 13.73; IR (Nujol,  $\text{cm}^{-1}$ ):  $\nu(\text{Os-Cl})$  287; ESI-MS (pos ion mode,  $\text{CH}_2\text{Cl}_2$ ):  $m/z = 647.2324$  ( $[\text{M-Cl}]^+$ ); Anal. Calcd for  $\text{C}_{30}\text{H}_{35}\text{ClN}_2\text{O}_2\text{Os}$  (681.30): C, 52.89; H, 5.18; N, 4.11; Found: C, 53.12; H, 5.36; N, 4.15 (%).

### Compound 3



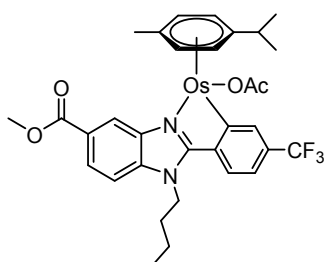
Yellow solid (47%).  $^1\text{H}$  NMR (600 MHz,  $\text{CDCl}_3$ )  $\delta$  8.40 (d,  $J = 1.3$  Hz, 1H), 8.01 (dd,  $J = 8.5, 1.4$  Hz, 1H), 7.72 (d,  $J = 2.5$  Hz, 1H), 7.64 (d,  $J = 8.6$  Hz, 1H), 7.35 (d,  $J = 8.5$  Hz, 1H), 6.63 (dd,  $J = 8.6, 2.5$  Hz, 1H), 5.88 (d,  $J = 5.4$  Hz, 1H), 5.72 (d,  $J = 5.4$  Hz, 1H), 5.62 (d,  $J = 5.4$  Hz, 1H), 5.34 (d,  $J = 5.4$  Hz, 1H), 4.54 (m, 1H), 4.43 (m, 1H), 4.00 (s, 3H), 3.92 (s, 3H), 2.25 (s, 3H), 1.90 (m, 2H), 1.43 (m, 2H), 0.96 (t,  $J = 7.3$  Hz, 3H), 0.92 (d,  $J = 6.9$  Hz, 3H), 0.74 (d,  $J = 6.9$  Hz, 3H);  $^{13}\text{C}$  NMR (151 MHz,  $\text{CDCl}_3$ )  $\delta$  171.98, 167.36, 163.13, 160.58, 140.7, 139.17, 126.22, 125.65, 125.2, 125.1, 124.42, 119.03, 109.58, 109.17, 95.18, 89.66, 79.94, 78.71, 72.94, 70.88, 55.26, 52.39, 44.74, 31.74, 31.35, 23.1, 22.1, 20.24, 18.9, 13.88; IR (Nujol,  $\text{cm}^{-1}$ ):  $\nu(\text{Os-Cl})$  289; ESI-MS (pos ion mode,  $\text{CH}_2\text{Cl}_2$ ):  $m/z = 663.2239$  ( $[\text{M-Cl}]^+$ ); Anal. Calcd for  $\text{C}_{30}\text{H}_{35}\text{ClN}_2\text{O}_3\text{Os}$  (697.30): C, 51.67; H, 5.06; N, 4.02; Found: C, 51.40; H, 4.89; N, 3.94 (%).

#### Compound 4



Yellow solid (52%),  $^1\text{H NMR}$  (600 MHz,  $\text{CDCl}_3$ )  $\delta$  8.43 (d,  $J = 1.2$  Hz, 1H), 8.05 (dd,  $J = 8.5, 1.5$  Hz, 1H), 7.88 (dd,  $J = 9.3, 2.6$  Hz, 1H), 7.68 (dd,  $J = 8.6, 5.3$  Hz, 1H), 7.39 (d,  $J = 8.5$  Hz, 1H), 6.76 (td,  $J = 8.6, 2.6$  Hz, 1H), 5.91 (d,  $J = 5.5$  Hz, 1H), 5.74 (d,  $J = 5.4$  Hz, 1H), 5.64 (d,  $J = 5.5$  Hz, 1H), 5.36 (d,  $J = 5.4$  Hz, 1H), 4.44 (m, 2H), 4.01 (s, 3H), 2.26 (m, 4H), 2.23 (m, 1H), 1.91 (quintet,  $J = 7.7$  Hz, 2H), 1.44 (m, 2H), 0.96 (t,  $J = 7.2$  Hz, 3H), 0.92 (d,  $J = 6.6$  Hz, 3H), 0.74 (d,  $J = 7.2$  Hz, 3H);  $^{13}\text{C NMR}$  (151 MHz,  $\text{CDCl}_3$ )  $\delta$  172.8, 172.8, 167.1, 163.9, 162.3, 140.4, 138.9, 129.3, 126.5, 126.4, 125.7, 125.6, 125.4, 124.7, 119.2, 110.0, 109.9, 109.8, 95.6, 90.2, 79.9, 78.9, 73.1, 70.9, 52.3, 44.7, 31.6, 31.2, 22.8, 21.9, 20.1, 18.7, 13.7;  $^{19}\text{F NMR}$  (282.40 MHz,  $\text{CDCl}_3$ )  $\delta$  -110.2; IR (Nujol,  $\text{cm}^{-1}$ ):  $\nu(\text{Os-Cl})$  285; ESI-MS (pos ion mode,  $\text{CH}_2\text{Cl}_2$ ):  $m/z = 651.2101$  ( $[\text{M-Cl}]^+$ ); Anal. Calcd for  $\text{C}_{29}\text{H}_{32}\text{ClF}_2\text{N}_2\text{O}_2\text{Os}$  (685.27): C, 50.83; H, 4.71; N, 4.09; Found: C, 50.76; H, 4.73; N, 4.06 (%).

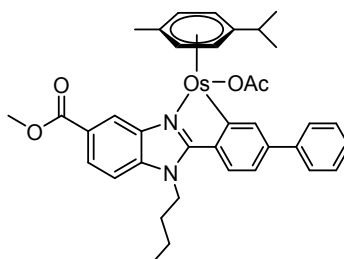
#### Compound 5



Yellow solid (62%)  $^1\text{H NMR}$  (600 MHz,  $\text{CDCl}_3$ )  $\delta$  8.73 (s, 1H), 8.63 (s, 1H), 8.12 (d,  $J = 8.6$  Hz, 1H), 7.75 (d,  $J = 8.0$  Hz, 1H), 7.43 (d,  $J = 8.6$  Hz, 1H), 7.33 (d,  $J = 8.0$  Hz, 1H), 6.11 (d,  $J = 5.4$  Hz, 1H), 5.93 (d,  $J = 5.4$  Hz, 1H), 5.84 (d,  $J = 5.2$  Hz, 1H), 5.53 (d,  $J = 5.2$  Hz, 1H), 4.58 (m, 2H), 4.02 (s, 3H), 2.16 (s, 3H), 2.06 (m, 1H), 1.91 (m, 2H), 1.60 (s, 3H, OAc), 1.42 (m, 2H), 0.98 (t,  $J = 7.3$  Hz, 3H), 0.80 (d,  $J = 6.8$  Hz, 3H), 0.65 (d,  $J = 6.8$  Hz, 3H);  $^{13}\text{C NMR}$  (151 MHz,  $\text{CDCl}_3$ )  $\delta$  176.9, 169.7, 167.1, 162.5, 141.2, 138.4, 137.0, 136.8, 125.7, 125.1, 123.4, 121.4, 119.6, 119.5, 109.7, 97.2, 86.2, 80.7, 78.1, 74.2,

69.3, 52.4, 44.8, 31.7, 31.6, 23.4, 23.2, 22.3, 20.0, 18.8, 13.7;  $^{19}\text{F}$  NMR (282.40 MHz,  $\text{CDCl}_3$ )  $\delta$  -62.1; ESI-MS (pos ion mode,  $\text{CH}_2\text{Cl}_2$ ):  $m/z = 701.2049$  ( $[\text{M}-\text{OAc}]^+$ ); Anal. Calcd for  $\text{C}_{32}\text{H}_{35}\text{F}_3\text{N}_2\text{O}_4\text{Os}$  (758.87): C, 50.65; H, 4.65; N, 3.69; Found: C, 50.69; H, 4.47; N, 3.58 (%).

### Compound 6



Greenish yellow solid (68%)  $^1\text{H}$  NMR (400 MHz,  $\text{CDCl}_3$ )  $\delta$  8.71 (d,  $J = 1.4$  Hz, 1H), 8.65 (d,  $J = 1.6$  Hz, 1H), 8.09 (dd,  $J = 8.6, 1.6$  Hz, 1H), 7.78 (dd,  $J = 8.4, 1.2$  Hz, 2H), 7.74 (d,  $J = 8.0$  Hz, 1H), 7.50 (t,  $J = 7.6$  Hz, 2H), 7.40 (d,  $J = 8.7$  Hz, 2H), 7.33 (dd,  $J = 8.0, 1.6$  Hz, 1H), 6.09 (d,  $J = 5.6$  Hz, 1H), 5.90 (t,  $J = 4.5$  Hz, 2H), 5.57 (d,  $J = 5.2$  Hz, 1H), 4.58 (m, 2H), 4.03 (s, 3H), 2.16 (s, 3H), 2.10 (m, 1H), 1.95 (m, 2H), 1.62 (s, 3H, OAc), 1.45 (m, 2H), 0.98 (t,  $J = 7.2$  Hz, 3H), 0.84 (d,  $J = 6.8$  Hz, 3H), 0.68 (d,  $J = 6.8$  Hz, 3H);  $^{13}\text{C}$  NMR (75 MHz,  $\text{CDCl}_3$ )  $\delta$  177.03, 169.84, 167.32, 163.50, 141.70, 141.32, 141.19, 139.26, 138.56, 132.75, 128.58, 127.57, 127.30, 125.21, 124.54, 123.89, 121.89, 120.88, 109.32, 96.29, 85.38, 80.64, 73.57, 69.38, 52.32, 44.64, 31.55, 23.47, 23.27, 22.19, 19.99, 18.80, 13.66; ESI-MS (pos ion mode,  $\text{CH}_2\text{Cl}_2$ ):  $m/z = 709.2429$  ( $[\text{M}-\text{OAc}]^+$ ); Anal. Calcd for  $\text{C}_{37}\text{H}_{40}\text{N}_2\text{O}_4\text{Os}$  (766.97): C, 57.94; H, 5.26; N, 3.65; Found: C, 58.03; H, 5.32; N, 3.48 (%).

## NMR spectra of compounds 1-6

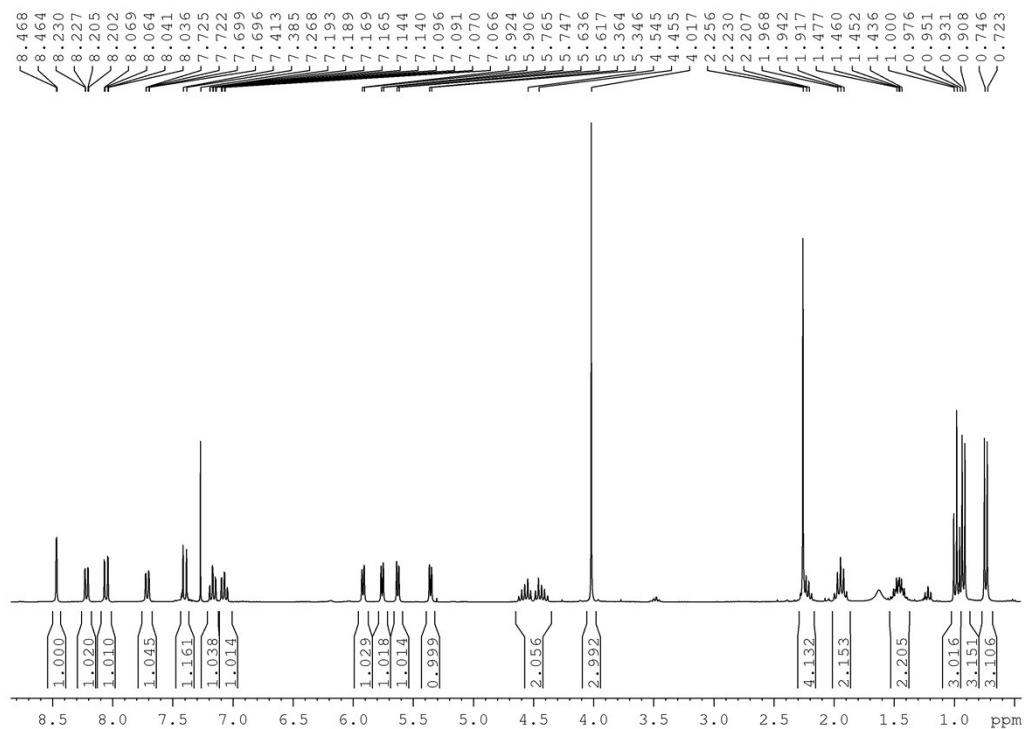


Figure S1.  $^1\text{H}$  NMR (300 MHz) spectrum of complex **1** in  $\text{CDCl}_3$ .

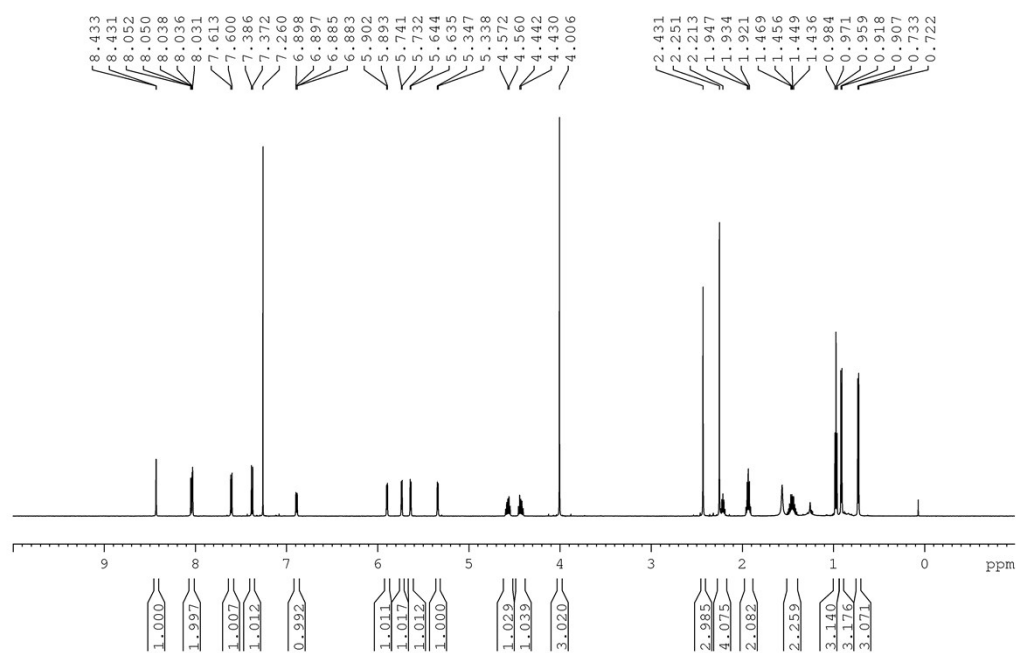
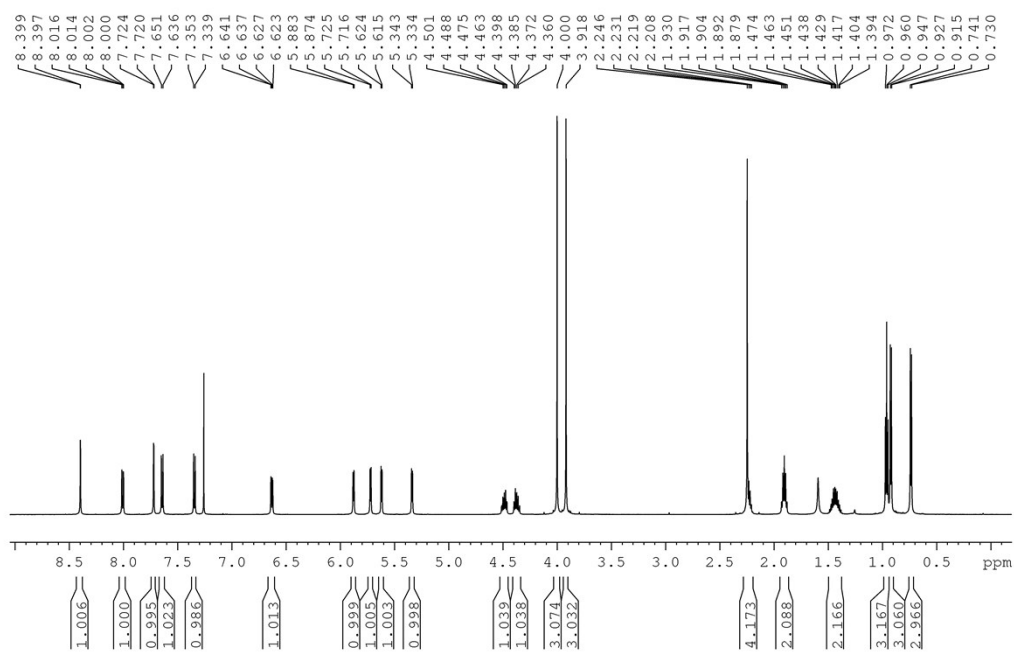
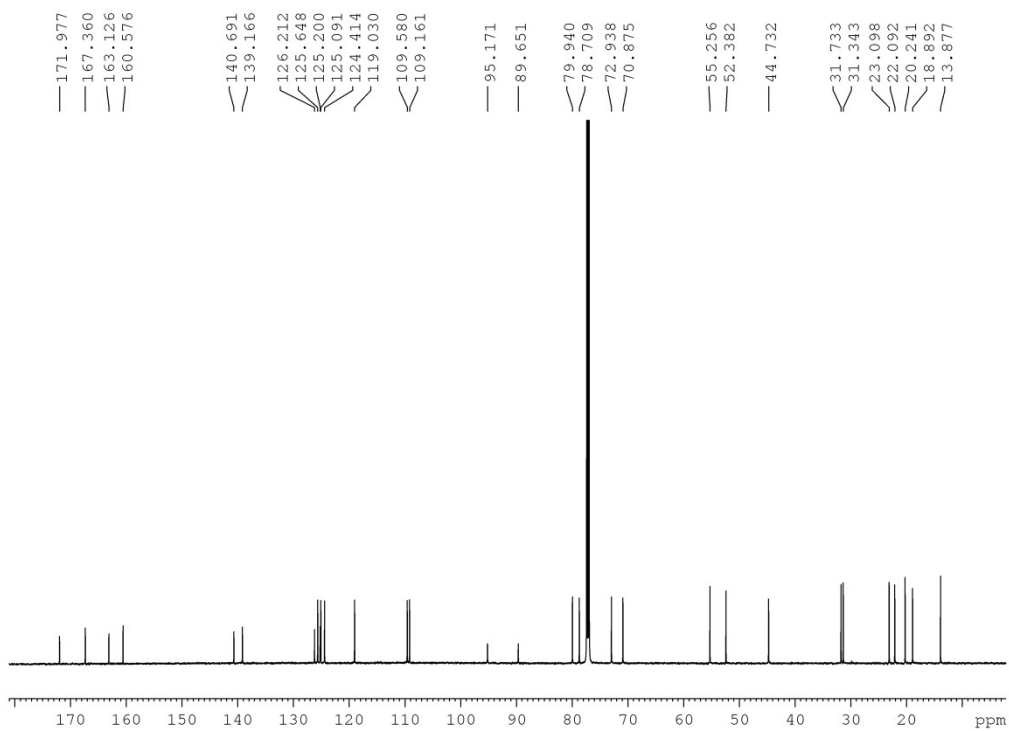


Figure S2.  $^1\text{H}$  NMR (600 MHz) spectrum of complex **2** in  $\text{CDCl}_3$ .



**Figure S3.**  $^1\text{H}$  NMR (600 MHz) spectrum of complex **3** in  $\text{CDCl}_3$ .



**Figure S4.**  $^{13}\text{C}$  NMR (151 MHz) spectrum of complex **3** in  $\text{CDCl}_3$ .

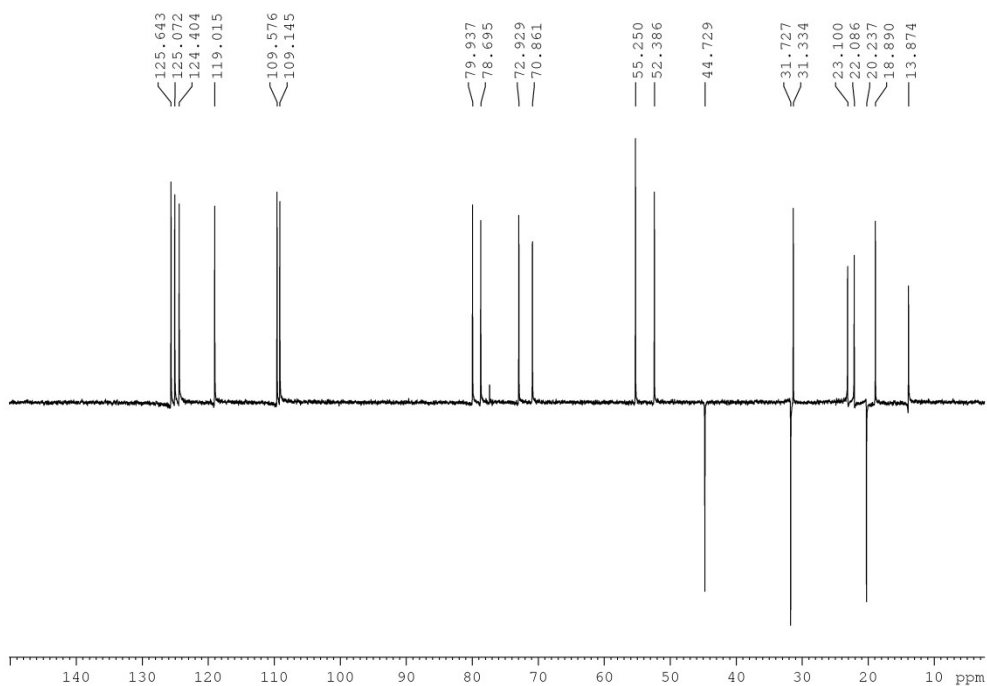


**Figure S5.** DEPT-135 NMR spectrum of complex **3** in  $\text{CDCl}_3$ .

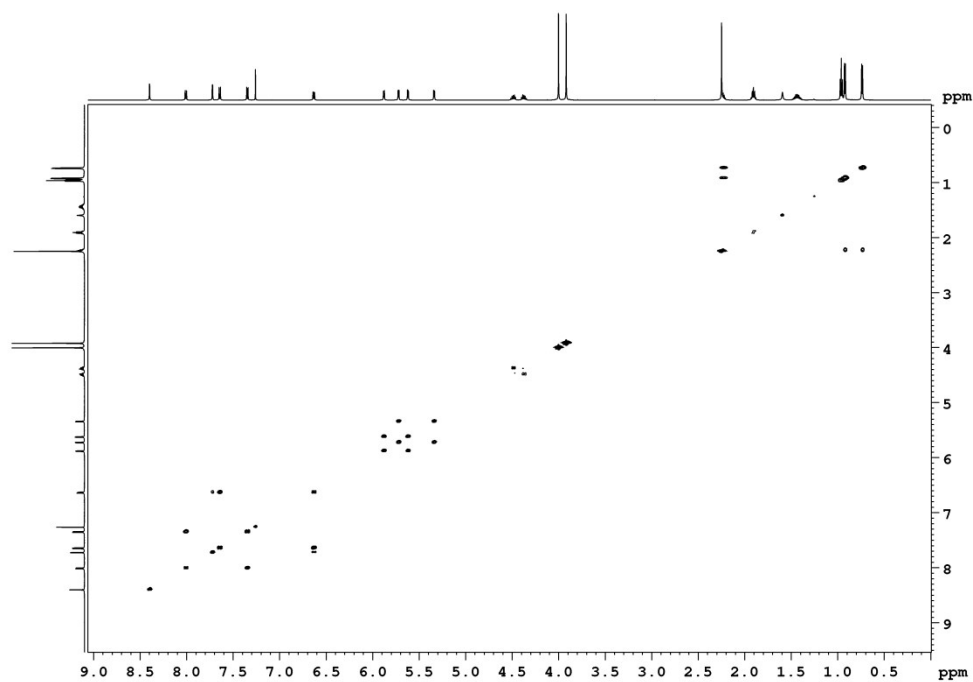


**Figure S6.**  $^1\text{H}$  COSY NMR spectrum of complex **3** in  $\text{CDCl}_3$ .

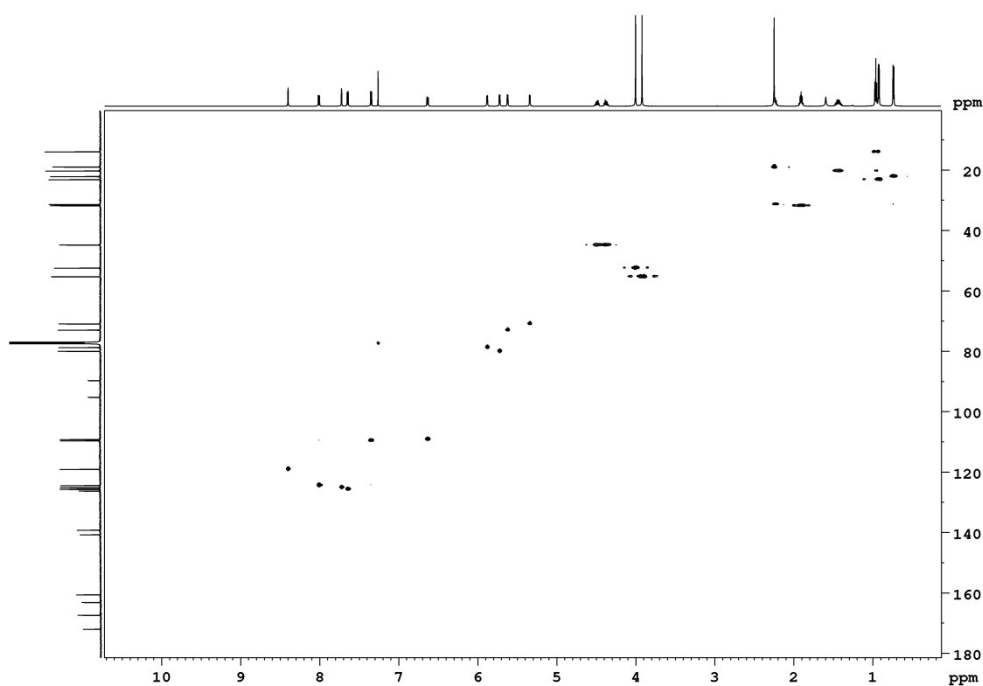


**Figure S7.**  $^1\text{H}$ - $^{13}\text{C}$  HSQC NMR spectrum of complex **3** in  $\text{CDCl}_3$ .

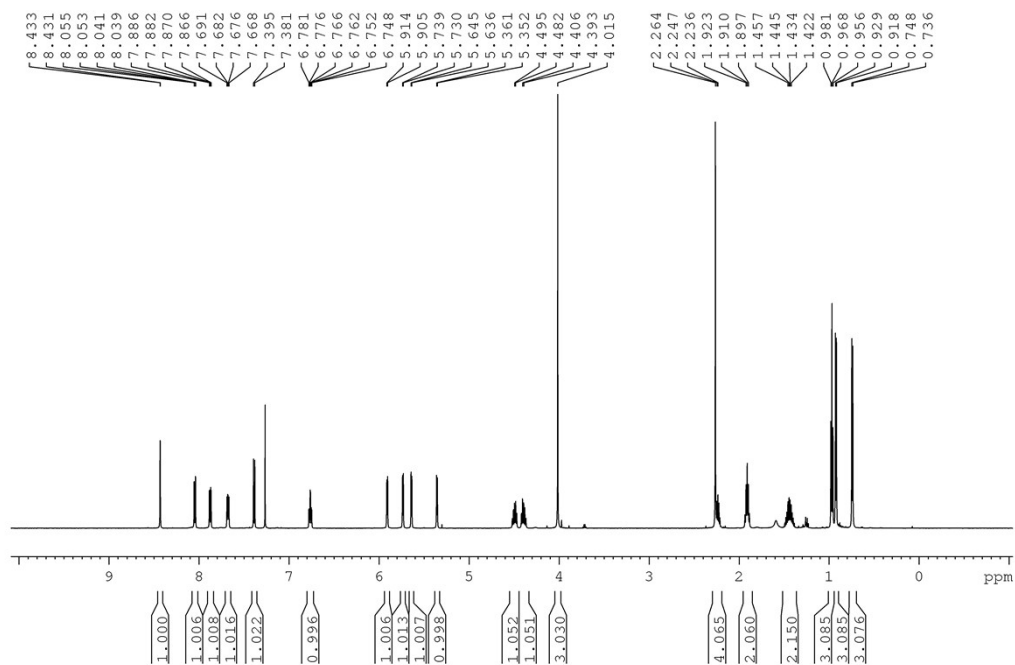


**Figure S8.**  $^1\text{H}$  NMR (600 MHz) spectrum of complex **4** in  $\text{CDCl}_3$ .

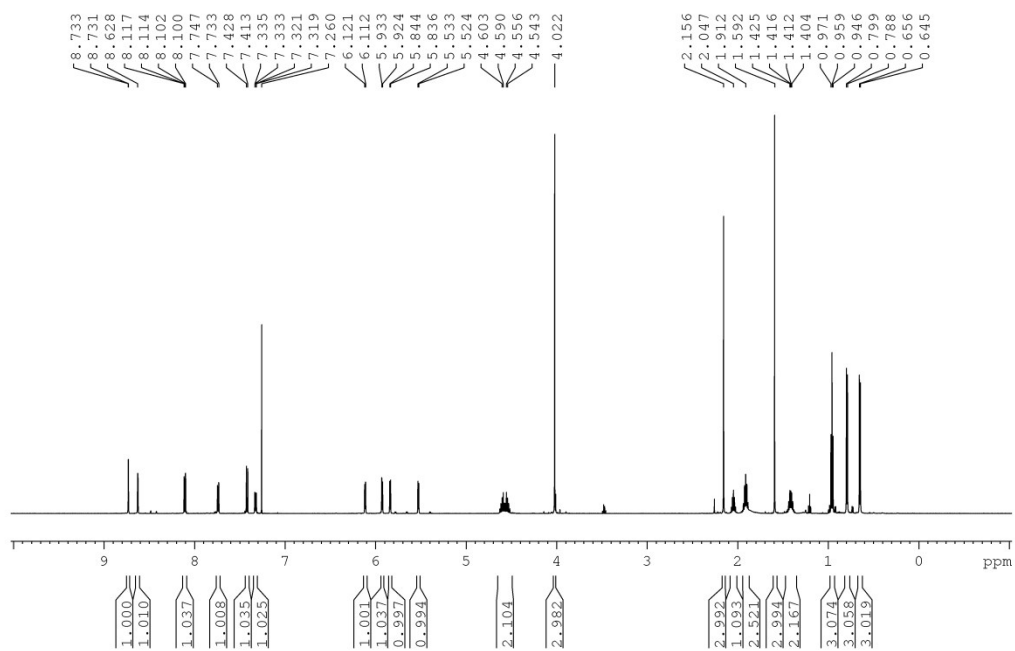


**Figure S9.**  $^1\text{H}$  NMR (600 MHz) spectrum of complex **5** in  $\text{CDCl}_3$ .

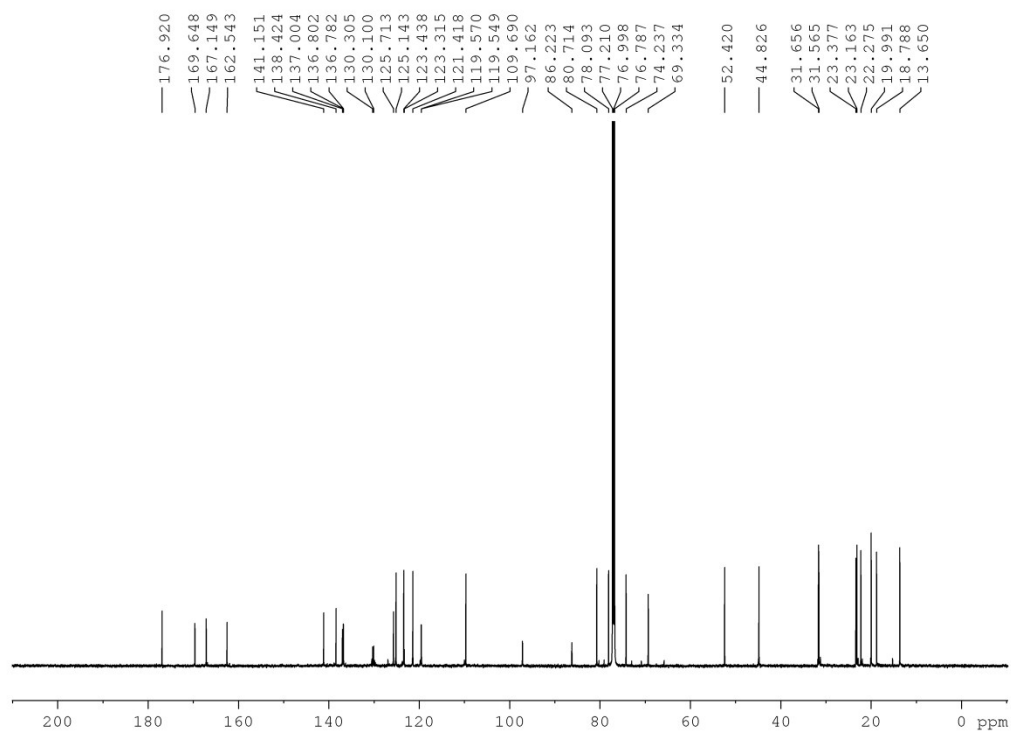


**Figure S10.**  $^{13}\text{C}$  NMR (151 MHz) spectra of complex **5** in  $\text{CDCl}_3$ .

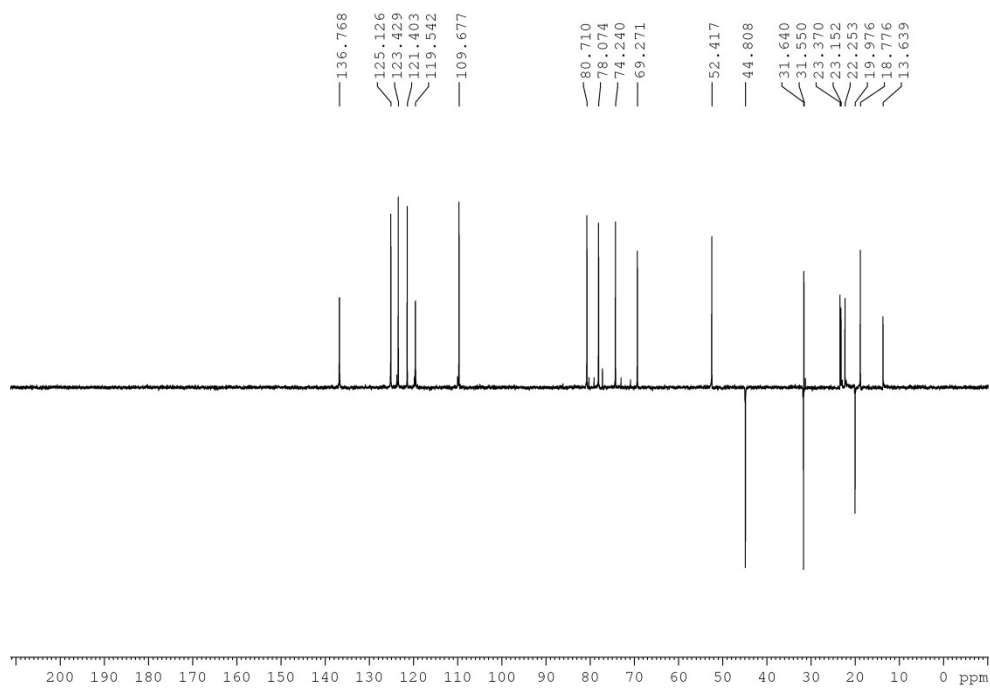


**Figure S11.** DEPT-135 NMR spectrum of complex **5** in CDCl<sub>3</sub>.

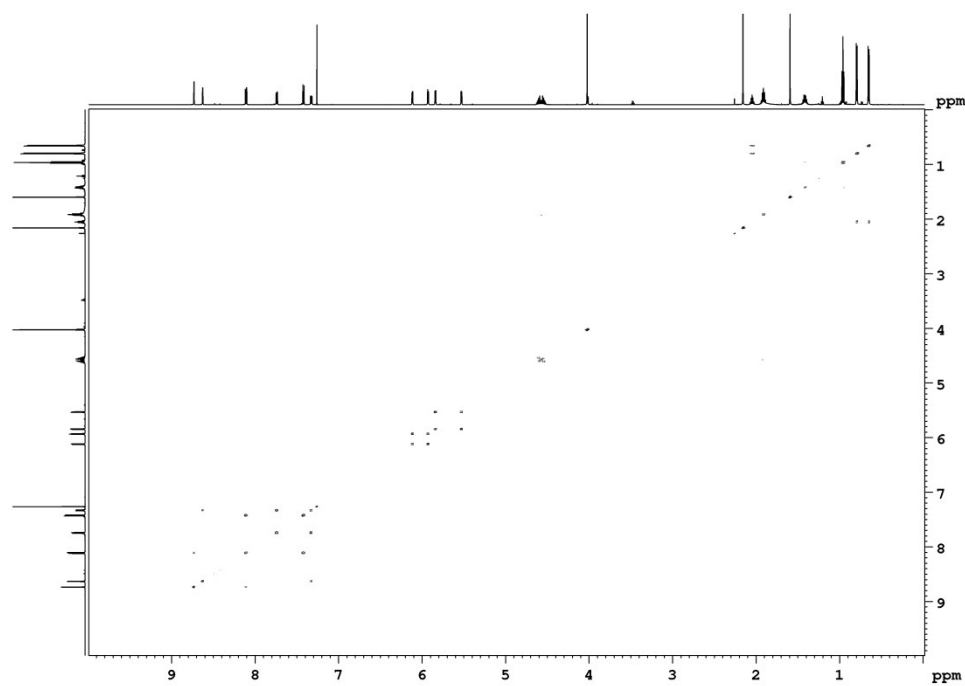


**Figure S12.** <sup>1</sup>H COSY NMR (600 MHz) spectra of complex **5** in CDCl<sub>3</sub>.

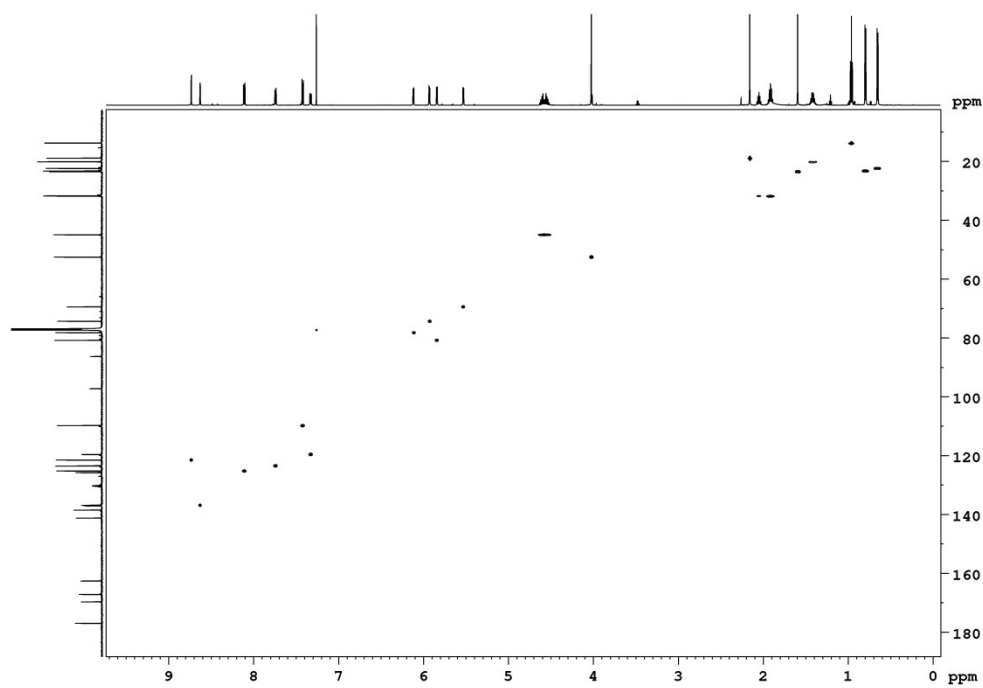


**Figure S13.**  $^1\text{H}$ - $^{13}\text{C}$  HSQC NMR spectrum of complex **5** in  $\text{CDCl}_3$ .

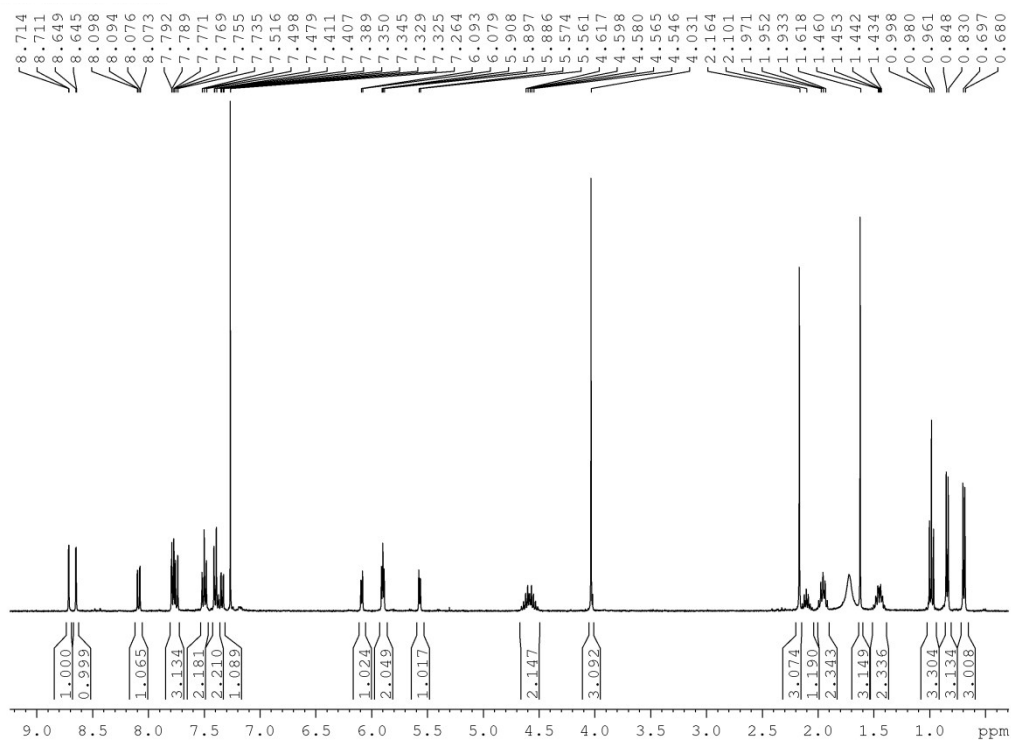


**Figure S14.**  $^1\text{H}$  NMR (400 MHz) spectrum of complex **6** in  $\text{CDCl}_3$ .

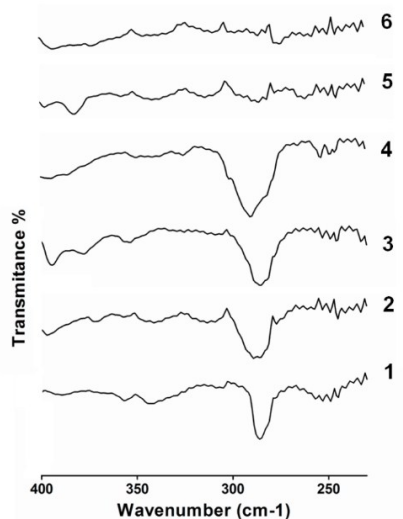


**Figure S15.** Portions of FT-IR spectra of complexes 1-6.

### Hydrolysis Studies

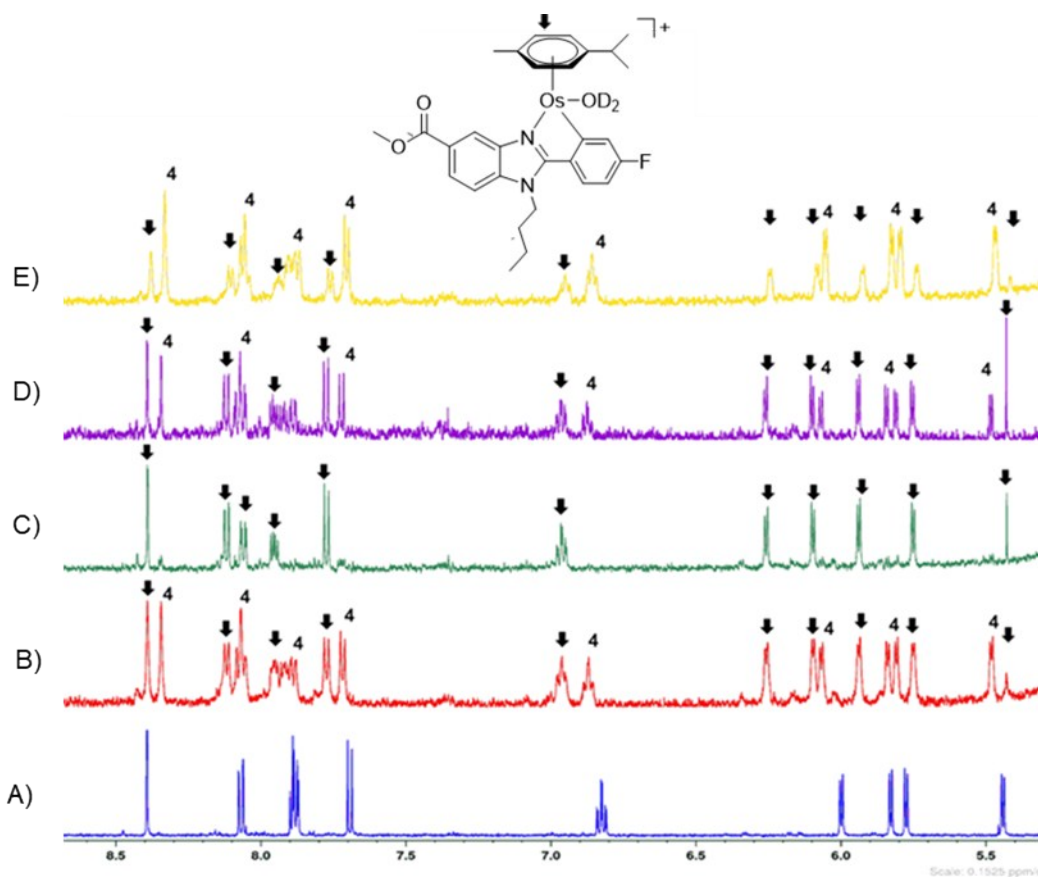


**Figure S16.**  $^1\text{H}$  NMR (600 MHz) spectra of complex 4 ( $\sim 0.5$  mM) in (A) MeOD- $d_4$ ; (B) 50% MeOD- $d_4$ / 50%  $\text{D}_2\text{O}$  (v/v) after 10 min; (C) 50% MeOD- $d_4$ / 50%  $\text{D}_2\text{O}$  (v/v) after 60 min; (D) after addition of 4 mM of NaCl to (C); (E) Spectrum of a new sample of complex 4 ( $\sim 0.5$  mM) and 4 mM of NaCl in 50% MeOD- $d_4$ / 50%  $\text{D}_2\text{O}$  after 10 min.

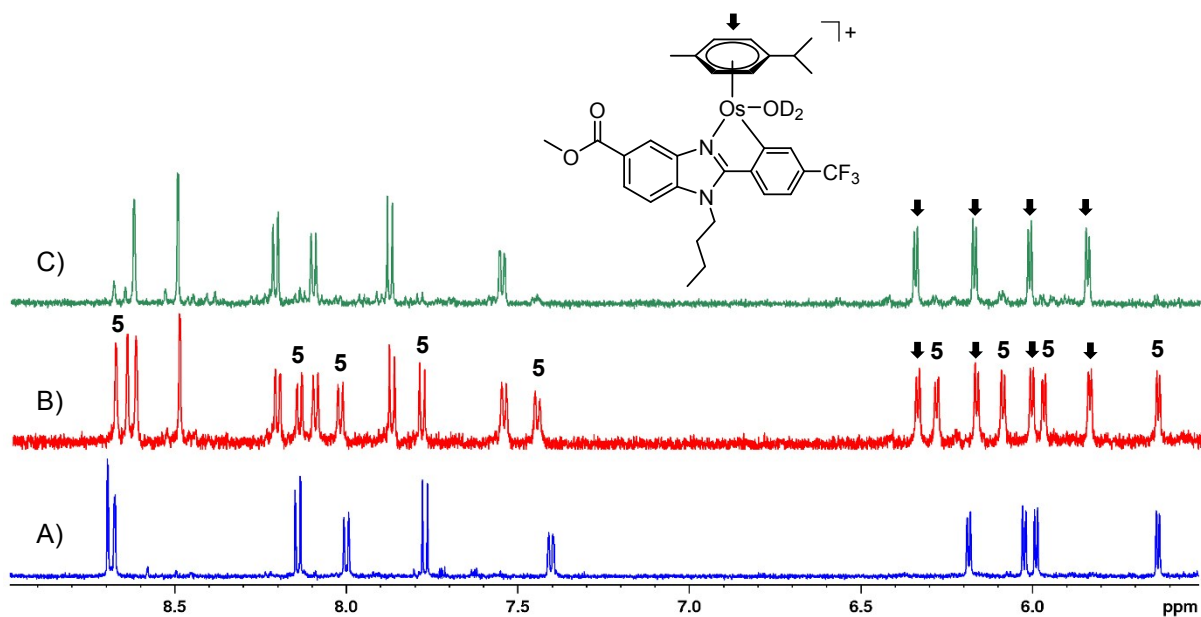


**Figure S17.**  $^1\text{H}$  NMR (600 MHz) spectra of complex **5** ( $\sim 0.5$  mM) in (A) MeOD- $d_4$ ; (B) 50% MeOD- $d_4$ / 50%  $\text{D}_2\text{O}$  (v/v) after 10 min. and (C) 50% MeOD- $d_4$ / 50%  $\text{D}_2\text{O}$  (v/v) after 30 min.

#### HPLC-MS stability study

The stability of the compound **2** in RPMI was analyzed using a RP-HPLC/MS TOF 6220 equipped with a double binary pump (model G1312A), degasser, autosampler (model G1329A), diode array detector (model G1315D) and mass detector in series Agilent Technologies 1200. Chromatographic analyses were carried out on a Brisa C18 column (150 mm x 4.6 mm, 5  $\mu\text{m}$  particle size). The mobile phase was a mixture of (A)  $\text{H}_2\text{O}/\text{HCOOH}$  0.1% and (B) acetonitrile/  $\text{HCOOH}$  0.1%. The flow rate was 0.6  $\text{mL}^{-1}$ . Chromatograms were recorded at 280 nm. The HPLC system was controlled by a ChemStation software (MASS HUNTER).

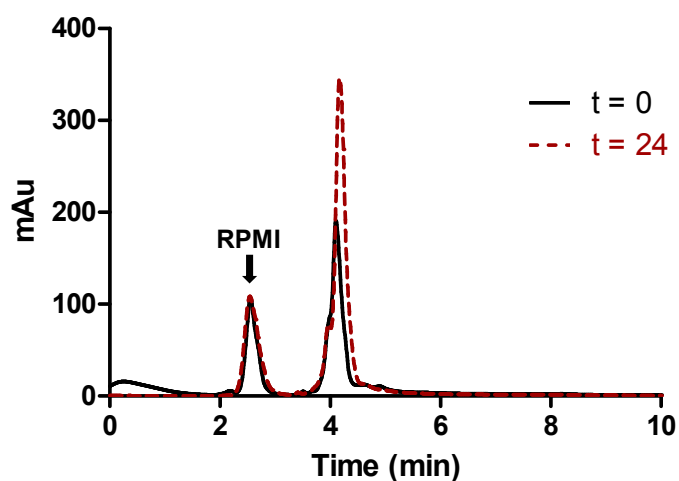


**Figure S18.** HPLC chromatograms of **2** (ca. 100  $\mu\text{M}$ ) in RPMI culture medium with 4% DMSO at  $t = 0$  h and  $t = 24$  h at room temperature.

#### Reaction with $\text{NAD}^+$

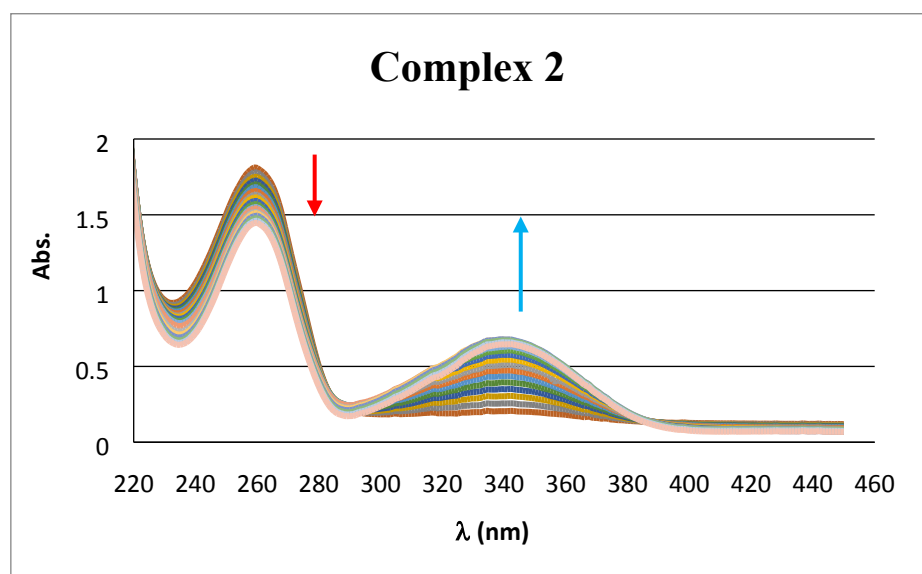


**Figure S19.** UV-Vis spectra of the reaction of  $\text{NAD}^+$  (100  $\mu\text{M}$ ),  $\text{HCOONa}$  (20 mM) with complex **2** (10  $\mu\text{M}$ ) in 10% MeOH / 90%  $\text{H}_2\text{O}$  (v/v) at 298 K for 5 hours. Spectra were recorded every 15 minutes.<sup>4</sup>

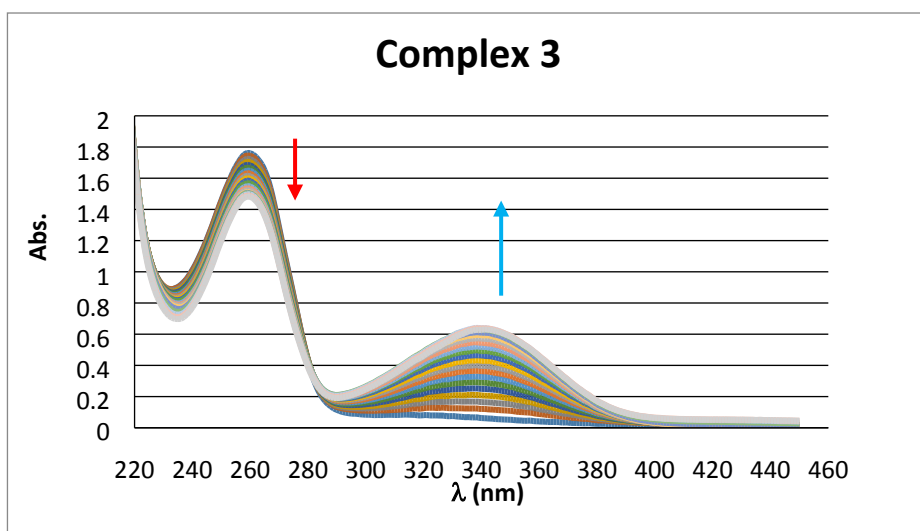


**Figure S20.** UV-Vis spectra of the reaction of NAD<sup>+</sup> (100 μM), HCOONa (20 mM) with complex 3 (10 μM) in 10% MeOH / 90% H<sub>2</sub>O (v/v) at 298 K for 5 h. Spectra were recorded every 15 min.<sup>4</sup>

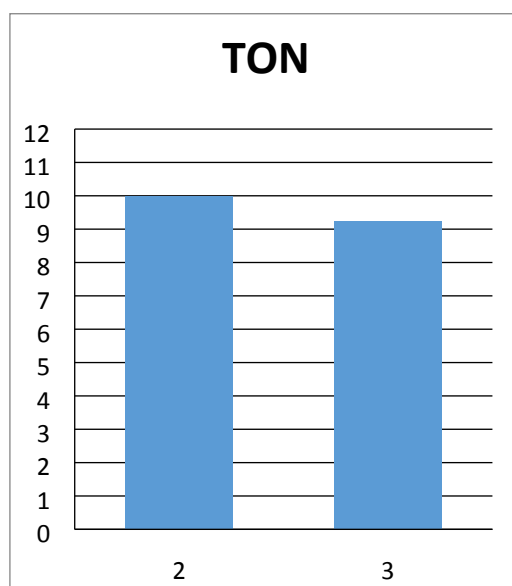


**Figure S21.** TON values of the compounds 2 and 3 at 4 h of the reaction of NAD<sup>+</sup> (100 μM), HCOONa (20 mM) with complex 2 (10 μM) in 10% MeOH / 90% H<sub>2</sub>O (v/v) at 298 K.<sup>4</sup>

### Cell lines and culture media

Human ovarian carcinoma A2780 and A2780cisR cell lines were grown in RPMI-1640, supplemented with 10% fetal bovine serum (FBS) and 2 mM L-glutamine. Breast cancer cells, MCF-7, and the non-tumorigenic BGM cells were grown in DMEM

containing 1 g/L glucose supplemented with 10% final concentration of FBS and 2 mM L-glutamine. The acquired resistance of A2780cisR cells was maintained by supplementing the medium with 1  $\mu$ M cisplatin every second passage. All cell lines were cultured in a humidified incubator at 310 K in a 5% CO<sub>2</sub> atmosphere and subcultured 2–3 times a week with an appropriate density. The cells lines were confirmed to be mycoplasma-free using Hoechst DNA staining method.<sup>5</sup>

The maximum % of DMSO used was 0.4 (except for cisplatin, water diluted) and the measurements were corrected with a control containing the same amount of DMSO.

### Cytotoxicity Assays

Impact of drug exposure on cell viability was determined using a 3-(4,5-dimethylthiazo-2-yl)-2,5-diphenyl-tetrazolium bromide (MTT)-based vitality assay. Cells were cultured in a 96-well plate at a density of  $5 \cdot 10^3$  cells/well in 100  $\mu$ L complete medium and allowed to attach overnight. Serial dilutions of chemical complexes were added at the final concentrations in the range of 0 to 80  $\mu$ M. After 48 h, the cells were treated with the 50  $\mu$ L MTT (0.5 mg/mL) and incubated for additional 4 h at 310 K. The medium in each well was removed and 100  $\mu$ L DMSO was added in order to solubilize the purple formazan crystals formed in active mitochondria. The absorbance was measured at 570 nm using a microplate reader (FLUOstar Omega). The IC<sub>50</sub> values were calculated based on the inhibitory rate curves using Equation 1

$$I = \frac{I_{max}}{1 + \left(\frac{IC_{50}}{C}\right)^n}$$

Where  $I$  represent the percentage inhibition of viability observed,  $I_{max}$  is the maximal inhibitory effect,  $IC_{50}$  is the concentration that inhibits 50% of maximal growth,  $C$  is the concentration of the compound and  $n$  is the slope of the semi-logarithmic dose-response sigmoidal curves. This non-linear fitting was performed using SigmaPlot 13.0 software. All compounds were tested at least in two independent studies with quadruplicate points.

The maximum % of DMSO used to dilute osmium complexes was 0.4 (except for cisplatin, water diluted) and the measurements were corrected with a control containing the same amount of DMSO.

**Table S1.** The selectivity factor for investigated complexes and cisplatin against BGM cell line.<sup>a</sup>

Cell line	A2780	A2780cisR	MCF-7	5178A2	HCCT116 <sup>wt</sup>	HCT116 <sup>-/-</sup>
<b>1</b>	3.9	4.2	3.2	.3	3.1	2.6
<b>2</b>	4.8	5.5	2.7	2.0	2.6	2.7
<b>3</b>	6.1	6.0	2.7	2.4	3.0	2.5
<b>4</b>	3.0	2.5	1.5	1.8	1.5	2.0
<b>5</b>	3.8	2.1	2.5	1.1	0.9	1.1
<b>6</b>	1.7	1.7	2.2	0.5	0.7	0.6
<b>Cisplatin</b>	6.7	0.2	0.2	3.6	1.0	0.5

<sup>a</sup> The degree of selectivity of the investigated Os complexes is expressed as IC<sub>50</sub> of Os complex in non-tumorigenic cells BGM/ IC<sub>50</sub> of the complex in cancer cell line using values from Table 1.

**Table S2.** The selectivity factor for investigated complexes and cisplatin against EA.hy926 cell line.<sup>b</sup>

	A2780	A2780cisR	MCF-7	5178A2	HCCT116 <sup>wt</sup>	HCT116 <sup>-/-</sup>
<b>1</b>	1.6	1.7	1.3	0.9	1.3	1.0
<b>2</b>	2.4	2.7	1.3	1.0	1.3	1.4
<b>3</b>	2.6	2.6	1.2	1.0	1.3	1.1
<b>4</b>	1.4	1.2	0.7	0.9	0.7	0.9
<b>5</b>	4.5	2.5	3.0	1.3	1.0	1.3
<b>6</b>	3.2	3.1	4.1	1.0	1.3	1.1
<b>Cisplatin</b>	3.8	0.1	0.1	1.8	0.6	1.0

<sup>b</sup> The degree of selectivity of the investigated Os complexes is expressed as IC<sub>50</sub> of Os complex in non-tumorigenic cells EA.hy926 / IC<sub>50</sub> of the complex in cancer cell line using values from Table 1.

### Apoptotic induction

The apoptotic rate of A2780 cells upon exposure of equitoxic concentration of osmium complexes was evaluated using the FITC-Annexin V/Propidium Iodide (PI) labelling method. Briefly, A2780 cells were seeded in 24-well plates at a density of 2·10<sup>5</sup> cells/well and incubated overnight. Osmium complexes or cisplatin were then added to final equitoxic concentration. After 48 h, the cells were harvested and washed twice with PBS. Cells were centrifuged, and the pellets were resuspended in 185 µL binding buffer. Then, 5 µL FITC-Annexin-V and 10 µL PI were added and the resuspended cell solution was left at room temperature in the dark for 15 min. Cells were analyzed by flow cytometry (Beckman CoulterEpics XL) and a total of 10 000 events were acquired in each sample, registering at 620 and 525 nm for PI and Annexin V, respectively, λ<sub>exc</sub> = 488 nm. Data were analyzed using FlowingSoftware version 2.5.1).

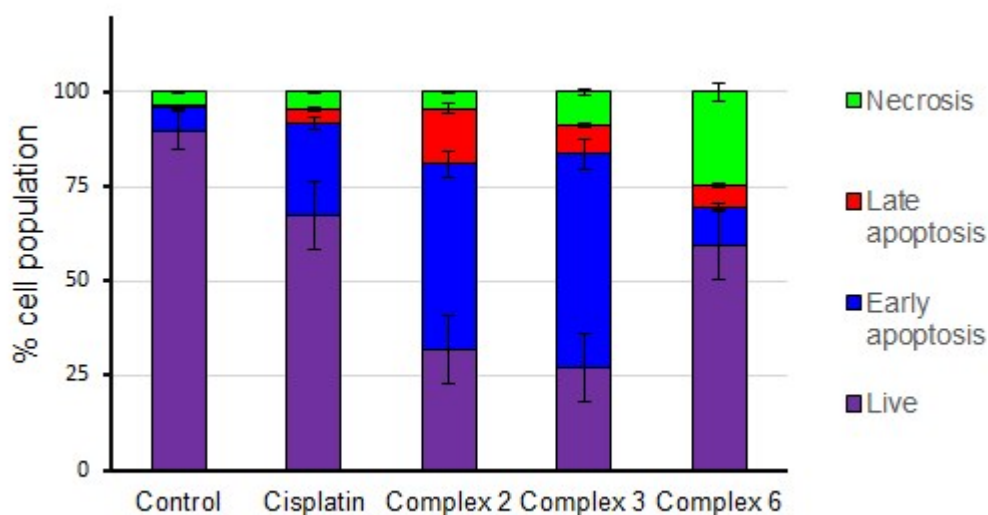


**Figure S22.** Bar charts of quantitative evaluation of apoptosis in A2780 after treatment with equitoxic concentrations of complexes **2**, **3**, **6** or cisplatin for 48 h.

#### **Mitochondrial polarization assay.**

Mitochondrial membrane potential was evaluated with the fluorescent probe Rhodamine-123 (Sigma-Aldrich). Briefly, A2780 ovarian cancer cells ( $2 \cdot 10^5$  per well) were seeded in 6-well plates and allowed to attach overnight. Then, compounds **2**, **3** or CDDP were added at a final equitoxic concentration and cells were incubated for additional 24 h. Carbonyl cyanide m-chlorophenyl hydrazone (CCCP) at  $10 \mu\text{M}$  was used as a positive control for membrane depolarization. After treatment, cells were collected and washed twice with PBS, Rhodamine-123 ( $1 \mu\text{M}$ ) was added and cells were incubated for 15 min at room temperature. In all samples, 10000 events were analyzed using a Beckman CoulterEpics XL flow cytometer ( $\lambda_{\text{exc}} = 488 \text{ nm}$  and  $\lambda_{\text{em}} = 530$ ). Data were analyzed using FlowingSoftware version 2.5.1.

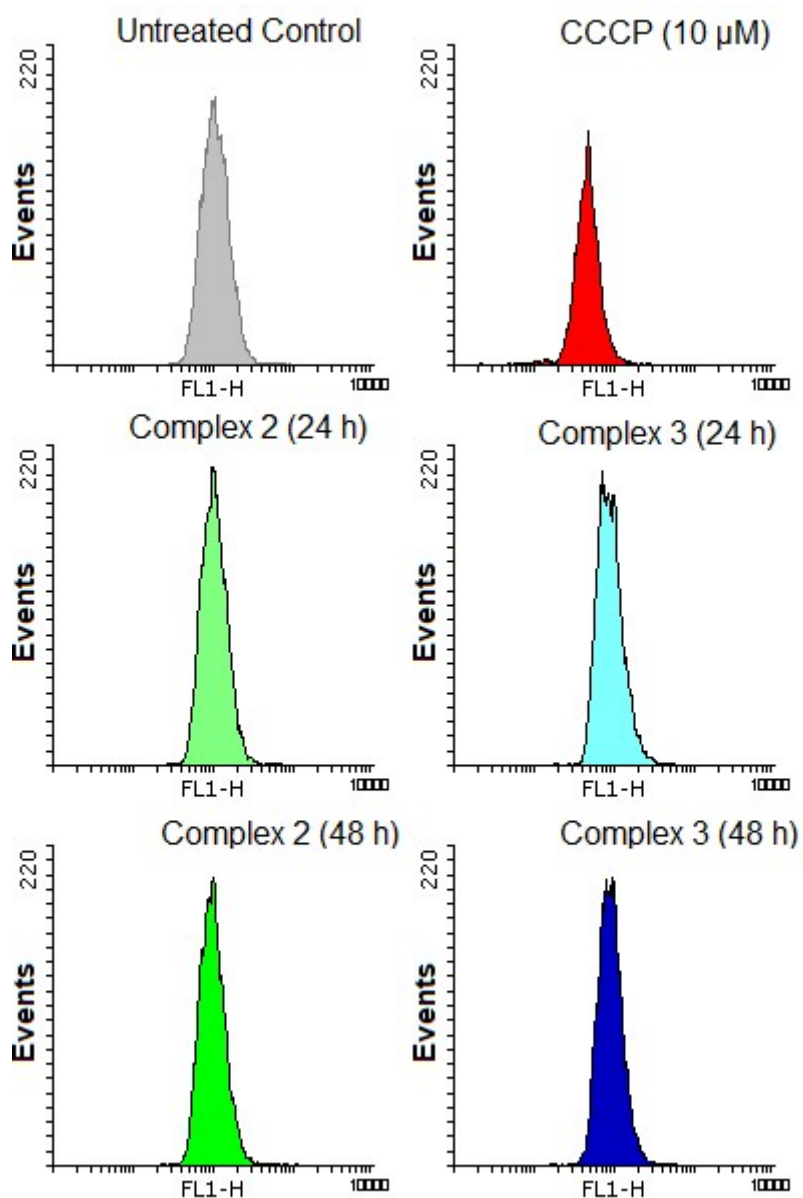


**Figure S23.** Effects of osmium complexes **2** and **3** on mitochondrial membrane potential at equitoxic concentrations determined by their  $IC_{50}$  on A2780 cells. FL1-H indicates fluorescence of Rhodamine-123 dye. Carbonyl cyanide *m*-chlorophenyl hydrazone (*CCCP*) was used as a positive control for membrane depolarization.

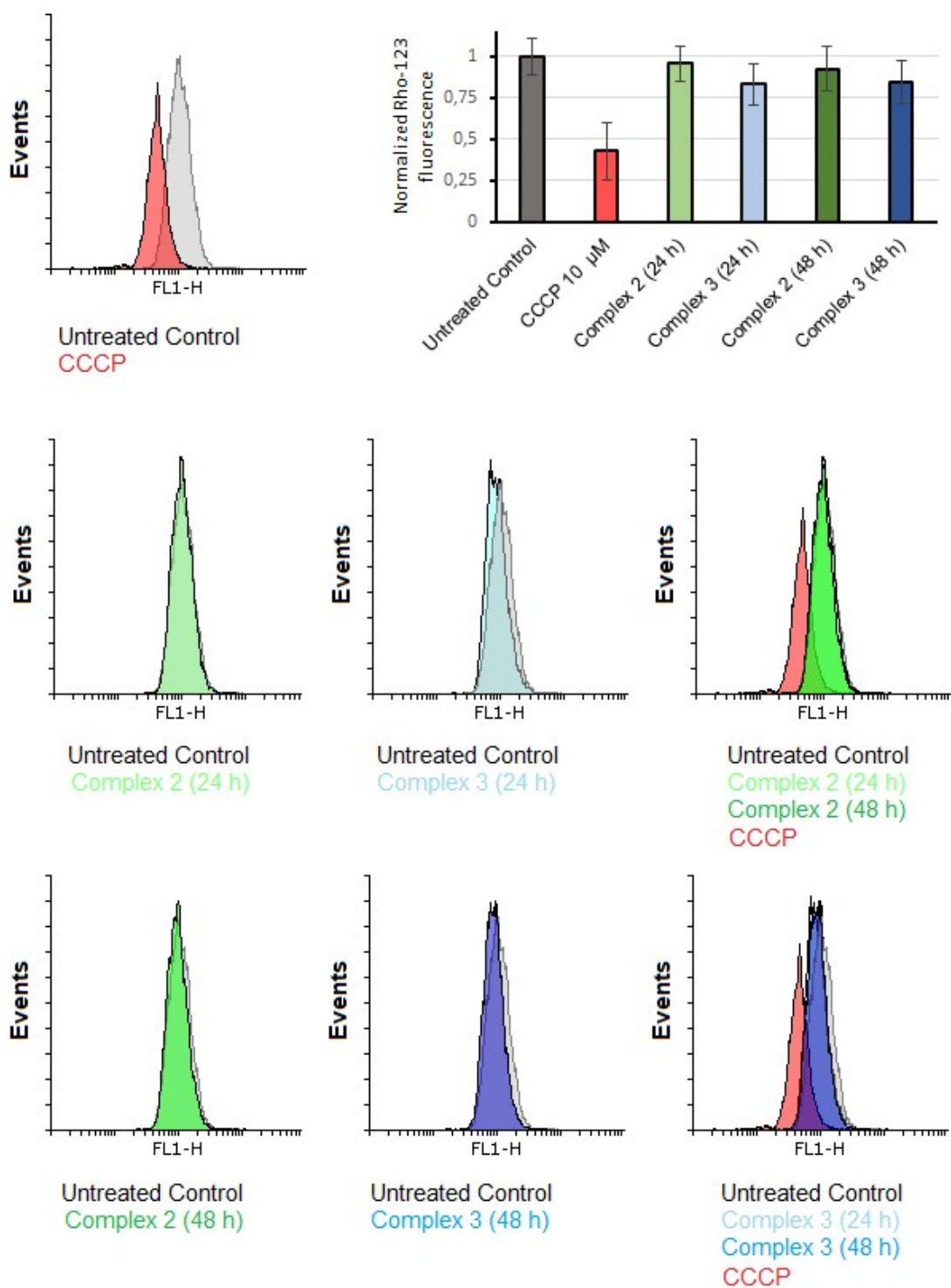


**Figure S24.** Effects of osmium complexes **2** and **3** on mitochondrial membrane potential at equitoxic concentrations determined by their  $IC_{50}$  on A2780 cells. FL1-H indicates fluorescence of Rhodamine-123 dye. Carbonyl cyanide m-chlorophenyl hydrazone (*CCCP*) was used as a positive control for membrane depolarization.

### Intracellular reactive oxygen species (ROS) determination.

The A2780 cells in the density of  $2 \times 10^4$  were seeded for 24 h in RPMI medium without Phenol Red on 96-well plates, and then treated with various concentrations (0-20  $\mu\text{M}$ ) of **2**, **3** or cisplatin for 24 h. Untreated cells contained maximal concentration of DMSO used in the treatment (0.4%). After the treatment, the cells were incubated with 10  $\mu\text{M}$  2',7'-dichlorodihydrofluorescein diacetate (DCFH-DA) for 30 min at 310 K. Cells were then washed with PBS and microplates scanned on a FLUOstar Omega spectrofluorometer measuring DCF oxidation product with excitation and emission wavelengths 488 nm and 530 nm, respectively. Alternatively, the generation of ROS was monitored by a DCFH-DA assay over 2 hours. Briefly,  $2 \times 10^4$  A2780 cells were seeded in 100  $\mu\text{L}$  of complete RPMI medium in 96-well plates and allowed to adhere to the plastic surface for 24 h at 310 K. The medium was aspirated by suction and cells were then incubated with 100  $\mu\text{L}$  of a 10  $\mu\text{M}$  DCFH-DA solution for 30 min at 310 K avoiding direct light. After the incubation, 100  $\mu\text{L}$  RPMI without phenol red containing diluted complex **2**, complex **3** or cisplatin (DMSO 0.4% for osmium complexes) was added to the cells. N-acetyl-cysteine (NAC) was used as a positive control for ROS scavenging. Fluorescence of DCF was measured over 2 hours every 5 min with FLUOstar Omega microplate reader. Experiments were performed in three independent repeats using triplicate points per concentration level.

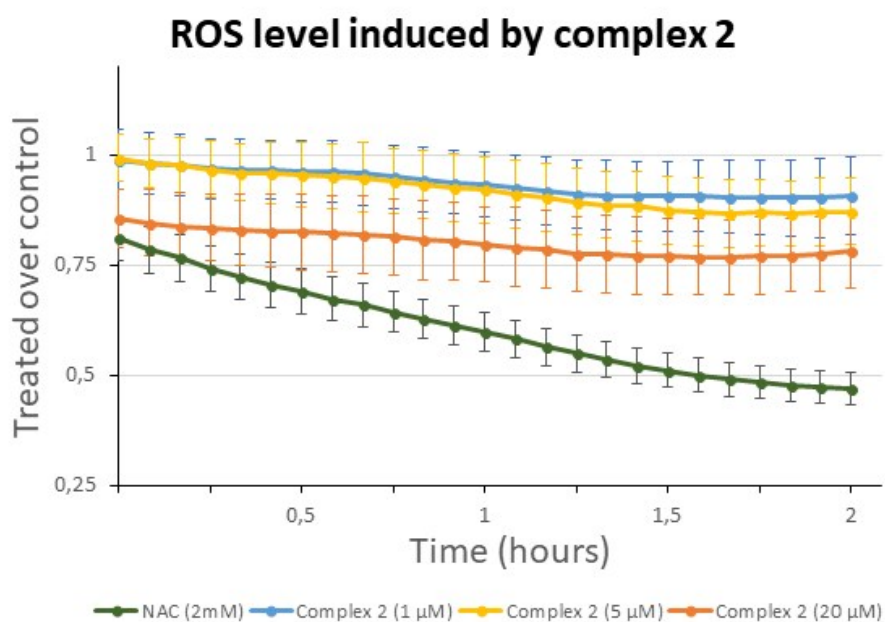


**Figure S25.** Level of reactive oxygen species (ROS) in A2780 cells upon treatment with complex 2 at different concentrations over 2 h compared to an untreated control. N-acetyl-cysteine (NAC) was used as a negative control.

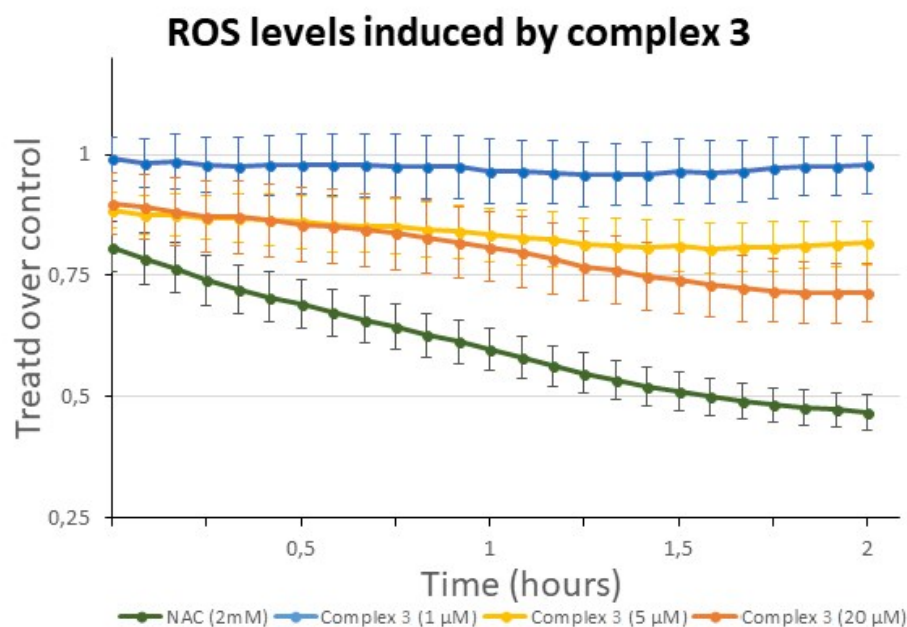


**Figure S26.** Level of reactive oxygen species (ROS) in A2780 cells upon treatment with complex 3 at different concentrations over 2 h compared to an untreated control. N-acetyl-cysteine (NAC) was used as a negative control.

### Cell cycle distribution perturbation

A2780 cells were seeded into 6-well plates at a density of  $2 \cdot 10^5$  cells per well. Cells were treated with either DMSO alone or with concentrations of the complex 2 or complex 3 determined by their  $IC_{50}$  values for 24 hours. Then cells were detached by trypsin, fixed in ice-cold ethanol for 30 min, followed by staining with propidium iodide (PI) for 1 h in the dark and analyzed using Beckman CoulterEpics cytometer ( $\lambda_{exc} = 488$  nm and  $\lambda_{em} = 530$ ).

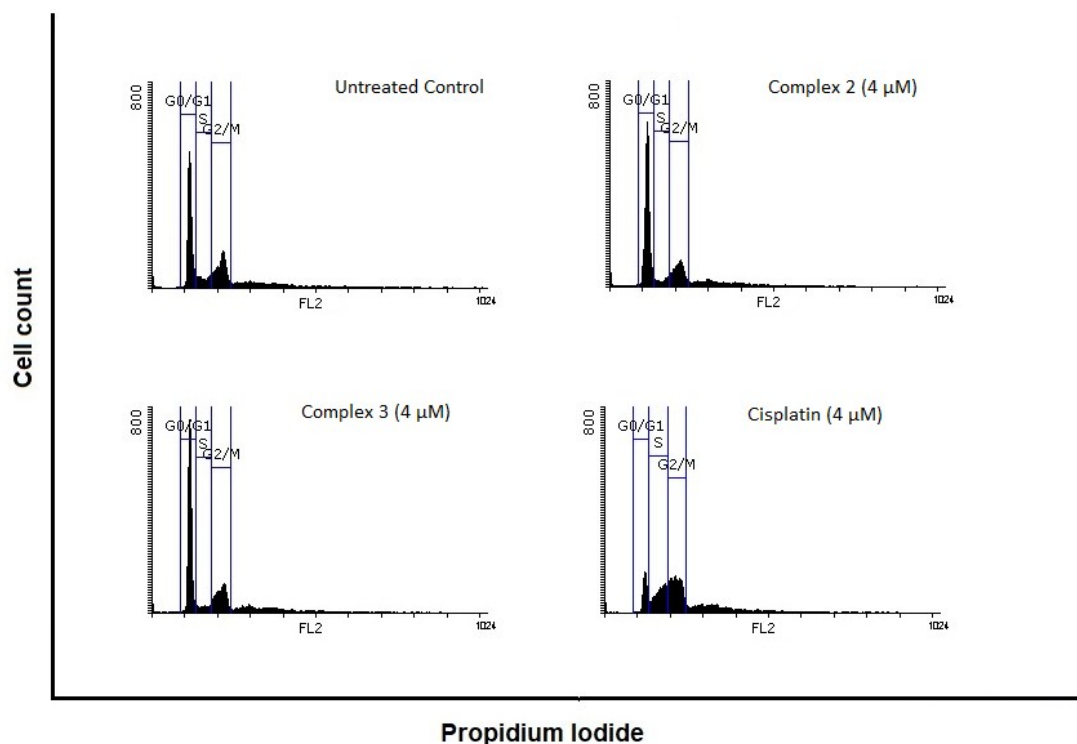


**Figure S27.** Flow cytometry analysis for cell cycle distribution of A2780 cancer cells exposed to compound **2**, **3** or cisplatin for 24 h at indicated concentration. Cell staining was performed by propidium iodide. Representative plots of two independent experiments are shown.

### Metal accumulation

Cell accumulation studies for osmium complexes were conducted on A2780 ovarian cancer cells. Briefly,  $1 \cdot 10^6$  cells were seeded on a 6-well plate. After 24 h of pre-incubation time in complete medium at 310 K, the complexes were added to give a final concentration of  $4 \mu\text{M}$  and a further 24 h of drug exposure was allowed. Cells were then treated with trypsin and counted. Cell pellets were digested using concentrated nitric acid 30 % and the amount of Osmium or Platinum was determined by Inductively Coupled Plasma Mass Spectrometry (ICP-MS).

A2780 cells were seeded and treated with complex **2**, complex **3** or cisplatin as described above and lysed in DNAzol reagent (DNAzol®, MRC) supplemented with RNase A ( $100 \text{ mg/mL}$ ). The DNA was precipitated using pure EtOH, washed with 75% EtOH and solubilized in  $8 \text{ mM NaOH}$ . The DNA content was quantified by UV spectrophotometry measuring  $A_{260}$  (NanoDrop ND-1000 spectrophotometer) and the amount of metal was determined by ICP-MS. Experiments were performed in duplicate.

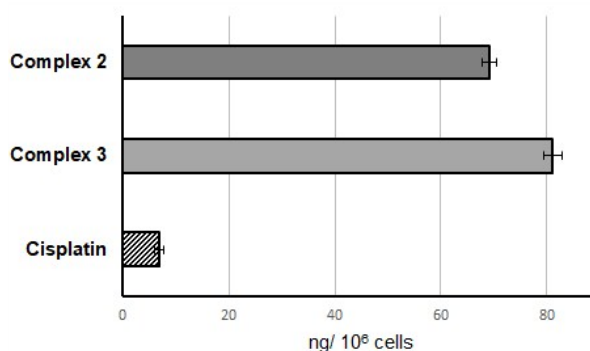


**Figure S28.** Metal accumulation of compounds **2**, **3** and cisplatin in A2780 cells treated for 24 h. Measurements indicate total cellular uptake of <sup>189</sup>Os for tested compounds and <sup>195</sup>Pt for cisplatin.

**Table S3.** Metal accumulation of **2**, **3** and cisplatin bound to DNA in A2780 cells treated for 24 h. Measurements indicate <sup>189</sup>Os for tested compounds and <sup>195</sup>Pt for cisplatin.

	pg /μg DNA
Complex 2	> 0.5
Complex 3	> 0.5
Cisplatin	10.3

### Tubulin polymerization assay

Wells of a 96 well μClear black well half area plate were filled with 50 μL of Brinkley's buffer 80 (20 % Glycerol and 3 mM of GTP) per well. Predilutions of **2**, **3**, **colchicine** as positive control and equal amounts of DMSO as negative control in H<sub>2</sub>O were added to reach working concentrations of 10 μM. Tubulin was added to each well (final concentration 5 μg/μl) and the OD<sub>340</sub> was instantly upon addition of tubulin using a preheated (37 °C) Tecan Infinite F200 plate reader. The results are representative for at least two repetitions of the assay.

## X-ray Crystallographic Analysis

Single crystals suitable for X-ray diffraction analysis were obtained for complexes **1** and **6** from CH<sub>2</sub>Cl<sub>2</sub>/ toluene/ hexane (2:1:3). Crystals were mounted on glass fibers and transferred to the cold gas stream of the diffractometer Bruker Smart APEX. Data were recorded with Mo K $\alpha$  radiation ( $\lambda = 0.71073$  Å) in  $\omega$  scan mode. Absorption correction for the compound was based on multi-scans.

Both structures were solved by direct methods (SHELXS-97);<sup>6</sup> refinement was done by full-matrix least squares on  $F^2$  using the SHELXL-97 program suite;<sup>6</sup> empirical (multi-scan) absorption correction with SADABS (Bruker).<sup>7</sup> All non-hydrogen positions were refined with anisotropic temperature factors. Hydrogen atoms for aromatic CH, aliphatic CH<sub>2</sub> and CH<sub>3</sub> groups were positioned geometrically (C–H = 0.95 Å for aromatic CH, C–H = 0.99 Å for CH<sub>2</sub>, C–H = 0.98 Å for CH<sub>3</sub>) and refined using a riding model (AFIX 43 for aromatic CH, AFIX 23 for CH<sub>2</sub>, AFIX 137 for CH<sub>3</sub>), with  $U_{\text{iso}}(\text{H}) = 1.2U_{\text{eq}}(\text{CH}, \text{CH}_2)$  and  $U_{\text{iso}}(\text{H}) = 1.5U_{\text{eq}}(\text{CH}_3)$ . Details of the X-ray structure determinations and refinements are provided in **Table S4** for **1** and **Table S5** for **6**. Selected bond lengths and angles of **1** and **6** are listed in **Table S6** for **1** and **Table S7** for **6**.

Graphics were drawn with DIAMOND (Version 4.4).<sup>8</sup>

The asymmetric unit of compound **6** contains also a half-occupied molecule of dichloromethane and a half-occupied molecule of toluene. The dichloromethane and toluene crystal solvent molecules share a common position (Fig. S30). They were both refined to half occupancy with PART commands. For toluene the PART -n command was used as the toluene molecule sits around the inversion center. The phenyl ring of the toluene molecule was refined as a rigid group using AFIX 66 1.39 to fit the following next six non-H atoms to a regular hexagon with C—C = 1.39 Å.

The single crystal X-ray data has been deposited as CCDC deposition numbers 1859533 (**1**) and 1859534 (**6**) with the Cambridge Crystallographic Data Centre from which it can be obtained upon request at [www.ccdc.cam.ac.uk/data\\_request/cif](http://www.ccdc.cam.ac.uk/data_request/cif).

**Table S4.** Crystal data and refinement details for chlorido-(1-methyl-4-iso-propylbenzene)-(N-n-butyl-(phenyl)(methylester)benzimidazol- $\kappa$ N,C)osmium(II), **1**.

### Crystal data

C <sub>29</sub> H <sub>33</sub> ClN <sub>2</sub> O <sub>2</sub> Os	$F(000) = 1320$
$M_r = 667.22$	$D_x = 1.796 \text{ Mg m}^{-3}$
Monoclinic, $P2_1/n$	Mo K $\alpha$ radiation, $\lambda = 0.71073$ Å

$a = 11.0472 (6) \text{ \AA}$	Cell parameters from 9768 reflections
$b = 19.7668 (10) \text{ \AA}$	$\theta = 2.7\text{--}30.5^\circ$
$c = 12.2934 (6) \text{ \AA}$	$\mu = 5.31 \text{ mm}^{-1}$
$\beta = 113.1612 (18)^\circ$	$T = 100 \text{ K}$
$V = 2468.1 (2) \text{ \AA}^3$	Prisms, yellow
$Z = 4$	$0.10 \times 0.09 \times 0.08 \text{ mm}$

### Data collection

Bruker D8 QUEST CCD diffractometer	7582 independent reflections
Radiation source: fine-focus sealed tube	6178 reflections with $I > 2\sigma(I)$
Graphite monochromator	$R_{\text{int}} = 0.077$
$\omega$ and $\phi$ scans	$\theta_{\text{max}} = 30.6^\circ$ , $\theta_{\text{min}} = 2.1^\circ$
Absorption correction: multi-scan (SADABS; Sheldrick, 1996)	$h = -15 \rightarrow 15$
$T_{\text{min}} = 0.648$ , $T_{\text{max}} = 0.746$	$k = -28 \rightarrow 28$
103770 measured reflections	$l = -17 \rightarrow 17$

### Refinement

Refinement on $F^2$	0 restraints
Least-squares matrix: full	Hydrogen site location: inferred from neighbouring sites
$R[F^2 > 2\sigma(F^2)] = 0.041$	H-atom parameters constrained
$wR(F^2) = 0.063$	$w = 1/[\sigma^2(F_o^2) + 15.4911P]$ where $P = (F_o^2 + 2F_c^2)/3$
$S = 1.08$	$(\Delta/\sigma)_{\text{max}} = 0.002$
7582 reflections	$\Delta_{\text{max}} = 2.45 \text{ e \AA}^{-3}$
321 parameters	$\Delta_{\text{min}} = -1.76 \text{ e \AA}^{-3}$

**Table S5.** Crystal data and refinement details for acetato-(1-methyl-4-iso-propyl-benzene)-(N-n-butyl-(4-bi-phenyl)(methyl-ester)benzimidazol-kN,C)osmium(II) hemi-dichloromethane, hemi-toluene solvate, **6**.

### Crystal data

$\text{C}_{37}\text{H}_{40}\text{N}_2\text{O}_4\text{Os} \cdot 0.5(\text{C}_7\text{H}_8) \cdot 0.5(\text{CH}_2\text{Cl}_2)$	$Z = 2$
$M_r = 855.44$	$F(000) = 860$
Triclinic, $P\bar{1}$	$D_x = 1.628 \text{ Mg m}^{-3}$
$a = 10.9559 (6) \text{ \AA}$	Mo $K\alpha$ radiation, $\lambda = 0.71073 \text{ \AA}$
$b = 10.9932 (6) \text{ \AA}$	Cell parameters from 9621 reflections
$c = 16.2594 (9) \text{ \AA}$	$\theta = 2.7\text{--}28.4^\circ$
$\alpha = 105.966 (2)^\circ$	$\mu = 3.78 \text{ mm}^{-1}$

$\beta = 102.536 (2)^\circ$	$T = 100 \text{ K}$
$\gamma = 103.578 (2)^\circ$	Block, orange
$V = 1745.05 (17) \text{ \AA}^3$	$0.21 \times 0.13 \times 0.13 \text{ mm}$

### Data collection

Bruker D8 QUEST CCD diffractometer	8746 independent reflections
Radiation source: fine-focus sealed tube	7910 reflections with $I > 2\sigma(I)$
Graphite monochromator	$R_{\text{int}} = 0.047$
$\omega$ and $\phi$ scans	$\theta_{\text{max}} = 28.4^\circ$ , $\theta_{\text{min}} = 2.0^\circ$
Absorption correction: multi-scan ( <i>SADABS</i> ; Sheldrick, 1996)	$h = -14 \rightarrow 14$
$T_{\text{min}} = 0.623$ , $T_{\text{max}} = 0.746$	$k = -14 \rightarrow 14$
85900 measured reflections	$l = -21 \rightarrow 21$

### Refinement

Refinement on $F^2$	0 restraints
Least-squares matrix: full	Hydrogen site location: inferred from neighbouring sites
$R[F^2 > 2\sigma(F^2)] = 0.027$	H-atom parameters constrained
$wR(F^2) = 0.053$	$w = 1/[\sigma^2(F_o^2) + (0.0112P)^2 + 3.9323P]$ where $P = (F_o^2 + 2F_c^2)/3$
$S = 1.12$	$(\Delta/\sigma)_{\text{max}} = 0.005$
8746 reflections	$\Delta_{\text{max}} = 2.00 \text{ e \AA}^{-3}$
482 parameters	$\Delta_{\text{min}} = -0.99 \text{ e \AA}^{-3}$

**Table S6.** Geometric parameters ( $\text{\AA}$ ,  $^\circ$ ) for **1**.

Os—C29	2.071 (4)	C10—H10B	0.9800
Os—N1	2.093 (3)	C10—H10C	0.9800
Os—C3	2.153 (4)	C11—C24	1.451 (5)
Os—C2	2.187 (4)	C12—C13	1.394 (5)
Os—C5	2.195 (4)	C12—C17	1.408 (5)
Os—C4	2.226 (4)	C13—C14	1.382 (5)
Os—C1	2.294 (4)	C13—H13	0.9500
Os—C6	2.298 (4)	C14—C15	1.404 (5)
Os—Cl	2.4164 (9)	C14—H14	0.9500
O1—C22	1.206 (5)	C15—C16	1.398 (5)
O2—C22	1.343 (5)	C15—C22	1.493 (5)
O2—C23	1.442 (5)	C16—C17	1.391 (5)

N1—C11	1.339 (5)	C16—H16	0.9500
N1—C17	1.390 (5)	C18—C19	1.537 (6)
N2—C11	1.368 (5)	C18—H18A	0.9900
N2—C12	1.387 (5)	C18—H18B	0.9900
N2—C18	1.470 (5)	C19—C20	1.521 (6)
C1—C6	1.408 (6)	C19—H19A	0.9900
C1—C2	1.424 (6)	C19—H19B	0.9900
C1—C7	1.501 (6)	C20—C21	1.515 (6)
C2—C3	1.419 (6)	C20—H20A	0.9900
C2—H2	0.9500	C20—H20B	0.9900
C3—C4	1.423 (6)	C21—H21A	0.9800
C3—H3	0.9500	C21—H21B	0.9800
C4—C5	1.422 (5)	C21—H21C	0.9800
C4—C8	1.515 (6)	C23—H23A	0.9800
C5—C6	1.433 (6)	C23—H23B	0.9800
C5—H5	0.9500	C23—H23C	0.9800
C6—H6	1.0000	C24—C25	1.410 (5)
C7—H7A	0.9800	C24—C29	1.420 (5)
C7—H7B	0.9800	C25—C26	1.381 (6)
C7—H7C	0.9800	C25—H25	0.9500
C8—C9	1.530 (6)	C26—C27	1.387 (6)
C8—C10	1.535 (6)	C26—H26	0.9500
C8—H8	1.0000	C27—C28	1.389 (6)
C9—H9A	0.9800	C27—H27	0.9500
C9—H9B	0.9800	C28—C29	1.407 (5)
C9—H9C	0.9800	C28—H28	0.9500
C10—H10A	0.9800		
C29—Os—N1	76.22 (14)	C4—C8—H8	107.7
C29—Os—C3	91.70 (16)	C9—C8—H8	107.7
N1—Os—C3	145.40 (14)	C10—C8—H8	107.7
C29—Os—C2	111.08 (15)	C8—C9—H9A	109.5
N1—Os—C2	172.64 (14)	C8—C9—H9B	109.5
C3—Os—C2	38.16 (15)	H9A—C9—H9B	109.5
C29—Os—C5	131.50 (14)	C8—C9—H9C	109.5
N1—Os—C5	96.44 (13)	H9A—C9—H9C	109.5

C3—Os—C5	67.37 (15)	H9B—C9—H9C	109.5
C2—Os—C5	79.46 (14)	C8—C10—H10A	109.5
C29—Os—C4	100.28 (15)	C8—C10—H10B	109.5
N1—Os—C4	111.74 (13)	H10A—C10—H10B	109.5
C3—Os—C4	37.88 (15)	C8—C10—H10C	109.5
C2—Os—C4	68.60 (15)	H10A—C10—H10C	109.5
C5—Os—C4	37.51 (15)	H10B—C10—H10C	109.5
C29—Os—C1	146.05 (15)	N1—C11—N2	111.5 (3)
N1—Os—C1	135.74 (14)	N1—C11—C24	116.6 (3)
C3—Os—C1	67.38 (16)	N2—C11—C24	131.5 (3)
C2—Os—C1	36.96 (15)	N2—C12—C13	131.2 (3)
C5—Os—C1	66.29 (14)	N2—C12—C17	106.7 (3)
C4—Os—C1	79.81 (15)	C13—C12—C17	122.1 (3)
C29—Os—C6	167.52 (15)	C14—C13—C12	116.5 (3)
N1—Os—C6	107.31 (13)	C14—C13—H13	121.7
C3—Os—C6	78.67 (15)	C12—C13—H13	121.7
C2—Os—C6	65.77 (15)	C13—C14—C15	122.1 (4)
C5—Os—C6	37.11 (14)	C13—C14—H14	118.9
C4—Os—C6	67.24 (15)	C15—C14—H14	118.9
C1—Os—C6	35.71 (14)	C16—C15—C14	121.2 (3)
C29—Os—C1	84.62 (11)	C16—C15—C22	117.6 (3)
N1—Os—C1	82.64 (9)	C14—C15—C22	121.2 (3)
C3—Os—C1	129.05 (11)	C17—C16—C15	117.1 (3)
C2—Os—C1	96.89 (11)	C17—C16—H16	121.4
C5—Os—C1	142.81 (11)	C15—C16—H16	121.4
C4—Os—C1	165.49 (10)	N1—C17—C16	131.0 (3)
C1—Os—C1	88.50 (11)	N1—C17—C12	108.1 (3)
C6—Os—C1	107.59 (11)	C16—C17—C12	120.9 (3)
C22—O2—C23	116.3 (3)	N2—C18—C19	111.0 (3)
C11—N1—C17	106.7 (3)	N2—C18—H18A	109.4
C11—N1—Os	117.7 (2)	C19—C18—H18A	109.4
C17—N1—Os	135.0 (3)	N2—C18—H18B	109.4
C11—N2—C12	106.9 (3)	C19—C18—H18B	109.4
C11—N2—C18	128.1 (3)	H18A—C18—H18B	108.0
C12—N2—C18	124.5 (3)	C20—C19—C18	114.5 (3)

C6—C1—C2	118.7 (4)	C20—C19—H19A	108.6
C6—C1—C7	121.7 (4)	C18—C19—H19A	108.6
C2—C1—C7	119.4 (4)	C20—C19—H19B	108.6
C6—C1—Os	72.3 (2)	C18—C19—H19B	108.6
C2—C1—Os	67.5 (2)	H19A—C19—H19B	107.6
C7—C1—Os	129.7 (3)	C21—C20—C19	113.2 (4)
C3—C2—C1	120.6 (4)	C21—C20—H20A	108.9
C3—C2—Os	69.6 (2)	C19—C20—H20A	108.9
C1—C2—Os	75.6 (2)	C21—C20—H20B	108.9
C3—C2—H2	119.7	C19—C20—H20B	108.9
C1—C2—H2	119.7	H20A—C20—H20B	107.8
Os—C2—H2	127.0	C20—C21—H21A	109.5
C2—C3—C4	122.1 (4)	C20—C21—H21B	109.5
C2—C3—Os	72.2 (2)	H21A—C21—H21B	109.5
C4—C3—Os	73.8 (2)	C20—C21—H21C	109.5
C2—C3—H3	119.0	H21A—C21—H21C	109.5
C4—C3—H3	119.0	H21B—C21—H21C	109.5
Os—C3—H3	127.1	O1—C22—O2	124.6 (4)
C5—C4—C3	116.0 (4)	O1—C22—C15	124.5 (4)
C5—C4—C8	121.7 (4)	O2—C22—C15	110.9 (3)
C3—C4—C8	122.1 (4)	O2—C23—H23A	109.5
C5—C4—Os	70.1 (2)	O2—C23—H23B	109.5
C3—C4—Os	68.3 (2)	H23A—C23—H23B	109.5
C8—C4—Os	136.2 (3)	O2—C23—H23C	109.5
C4—C5—C6	122.7 (3)	H23A—C23—H23C	109.5
C4—C5—Os	72.4 (2)	H23B—C23—H23C	109.5
C6—C5—Os	75.3 (2)	C25—C24—C29	122.2 (3)
C4—C5—H5	118.6	C25—C24—C11	126.4 (4)
C6—C5—H5	118.6	C29—C24—C11	111.3 (3)
Os—C5—H5	125.4	C26—C25—C24	119.2 (4)
C1—C6—C5	119.6 (4)	C26—C25—H25	120.4
C1—C6—Os	72.0 (2)	C24—C25—H25	120.4
C5—C6—Os	67.5 (2)	C25—C26—C27	120.1 (4)
C1—C6—H6	119.2	C25—C26—H26	119.9
C5—C6—H6	119.2	C27—C26—H26	119.9

Os—C6—H6	119.2	C26—C27—C28	120.5 (4)
C1—C7—H7A	109.5	C26—C27—H27	119.7
C1—C7—H7B	109.5	C28—C27—H27	119.7
H7A—C7—H7B	109.5	C27—C28—C29	122.1 (4)
C1—C7—H7C	109.5	C27—C28—H28	119.0
H7A—C7—H7C	109.5	C29—C28—H28	119.0
H7B—C7—H7C	109.5	C28—C29—C24	115.9 (3)
C4—C8—C9	114.5 (4)	C28—C29—Os	125.7 (3)
C4—C8—C10	107.8 (3)	C24—C29—Os	118.2 (3)
C9—C8—C10	111.3 (4)		

**Table S7.** Geometric parameters (Å, °) for **6**.

Os—C29	2.077 (3)	C19—C20	1.530 (4)
Os—N5	2.086 (2)	C19—H19A	0.9900
Os—O3	2.099 (2)	C19—H19B	0.9900
Os—C3	2.148 (3)	C20—C21	1.527 (4)
Os—C5	2.167 (3)	C20—H20A	0.9900
Os—C2	2.188 (3)	C20—H20B	0.9900
Os—C4	2.198 (3)	C21—H21A	0.9800
Os—C1	2.243 (3)	C21—H21B	0.9800
Os—C6	2.265 (3)	C21—H21C	0.9800
O1—C22	1.206 (4)	C23—H23A	0.9800
O2—C22	1.340 (4)	C23—H23B	0.9800
O2—C23	1.446 (3)	C23—H23C	0.9800
O3—C36	1.292 (3)	C24—C25	1.402 (4)
O4—C36	1.231 (4)	C24—C29	1.415 (4)
N5—C11	1.338 (3)	C25—C26	1.382 (4)
N5—C17	1.385 (3)	C25—H25	0.9500
N8—C11	1.371 (3)	C26—C27	1.400 (4)
N8—C12	1.379 (3)	C26—H26	0.9500
N8—C18	1.473 (3)	C27—C28	1.401 (4)
C1—C6	1.418 (4)	C27—C30	1.492 (4)
C1—C2	1.432 (4)	C28—C29	1.402 (4)
C1—C7	1.494 (4)	C28—H28	0.9500
C2—C3	1.414 (4)	C30—C35	1.393 (4)

C2—H2	0.9500	C30—C31	1.398 (4)
C3—C4	1.430 (4)	C31—C32	1.390 (4)
C3—H3	0.9500	C31—H31	0.9500
C4—C5	1.421 (4)	C32—C33	1.377 (5)
C4—C8	1.518 (4)	C32—H32	0.9500
C5—C6	1.426 (4)	C33—C34	1.380 (5)
C5—H5	0.9500	C33—H33	0.9500
C6—H6	0.9500	C34—C35	1.394 (4)
C7—H7A	0.9800	C34—H34	0.9500
C7—H7B	0.9800	C35—H35	0.9500
C7—H7C	0.9800	C36—C37	1.509 (5)
C8—C10	1.517 (4)	C37—H37A	0.9800
C8—C9	1.533 (5)	C37—H37B	0.9800
C8—H8	1.0000	C37—H37C	0.9800
C9—H9A	0.9800	C38—C11	1.746 (11)
C9—H9B	0.9800	C38—C12	1.767 (10)
C9—H9C	0.9800	C38—H38A	0.9900
C10—H10A	0.9800	C38—H38B	0.9900
C10—H10B	0.9800	C39—C40	1.3900
C10—H10C	0.9800	C39—C44	1.3900
C11—C24	1.447 (4)	C39—C45	1.591(18)
C12—C13	1.398 (4)	C40—C41	1.3900
C12—C17	1.403 (4)	C40—H40	0.9500
C13—C14	1.383 (4)	C41—C42	1.3900
C13—H13	0.9500	C41—H41	0.9500
C14—C15	1.408 (4)	C42—C43	1.3900
C14—H14	0.9500	C42—H42	0.9500
C15—C16	1.391 (4)	C43—C44	1.3900
C15—C22	1.484 (4)	C43—H43	0.9500
C16—C17	1.389 (4)	C44—H44	0.9500
C16—H16	0.9500	C45—H45A	0.9800
C18—C19	1.526 (4)	C45—H45B	0.9800
C18—H18A	0.9900	C45—H45C	0.9800
C18—H18B	0.9900		

C29—Os—N5	76.20 (9)	C16—C15—C22	121.1 (3)
C29—Os—O3	88.85 (9)	C14—C15—C22	117.5 (3)
N5—Os—O3	81.81 (8)	C17—C16—C15	117.4 (3)
C29—Os—C3	90.67 (10)	C17—C16—H16	121.3
N5—Os—C3	138.80(10)	C15—C16—H16	121.3
O3—Os—C3	137.63(10)	N5—C17—C16	130.8 (3)
C29—Os—C5	133.36(11)	N5—C17—C12	108.1 (2)
N5—Os—C5	92.87 (10)	C16—C17—C12	121.1 (2)
O3—Os—C5	135.02(10)	N8—C18—C19	111.1 (2)
C3—Os—C5	68.05 (11)	N8—C18—H18A	109.4
C29—Os—C2	108.36(11)	C19—C18—H18A	109.4
N5—Os—C2	173.27(10)	N8—C18—H18B	109.4
O3—Os—C2	102.98(10)	C19—C18—H18B	109.4
C3—Os—C2	38.06 (11)	H18A—C18—H18B	108.0
C5—Os—C2	80.40 (11)	C18—C19—C20	113.1 (2)
C29—Os—C4	100.78(11)	C18—C19—H19A	109.0
N5—Os—C4	105.25(10)	C20—C19—H19A	109.0
O3—Os—C4	169.13 (9)	C18—C19—H19B	109.0
C3—Os—C4	38.40 (11)	C20—C19—H19B	109.0
C5—Os—C4	37.98 (11)	H19A—C19—H19B	107.8
C2—Os—C4	69.33 (11)	C21—C20—C19	113.4 (3)
C29—Os—C1	143.11(11)	C21—C20—H20A	108.9
N5—Os—C1	139.23(10)	C19—C20—H20A	108.9
O3—Os—C1	87.66 (10)	C21—C20—H20B	108.9
C3—Os—C1	68.28 (11)	C19—C20—H20B	108.9
C5—Os—C1	67.69 (11)	H20A—C20—H20B	107.7
C2—Os—C1	37.68 (11)	C20—C21—H21A	109.5
C4—Os—C1	81.61 (11)	C20—C21—H21B	109.5
C29—Os—C6	168.82(11)	H21A—C21—H21B	109.5
N5—Os—C6	107.79(10)	C20—C21—H21C	109.5
O3—Os—C6	101.99(10)	H21A—C21—H21C	109.5
C3—Os—C6	79.49 (11)	H21B—C21—H21C	109.5
C5—Os—C6	37.47 (11)	O1—C22—O2	123.0 (3)
C2—Os—C6	66.80 (10)	O1—C22—C15	124.7 (3)
C4—Os—C6	68.18 (11)	O2—C22—C15	112.3 (2)

C1—Os—C6	36.65 (10)	O2—C23—H23A	109.5
C22—O2—C23	115.2 (2)	O2—C23—H23B	109.5
C36—O3—Os	125.70(19)	H23A—C23—H23B	109.5
C11—N5—C17	107.0 (2)	O2—C23—H23C	109.5
C11—N5—Os	117.90(17)	H23A—C23—H23C	109.5
C17—N5—Os	134.88(18)	H23B—C23—H23C	109.5
C11—N8—C12	107.2 (2)	C25—C24—C29	121.4 (2)
C11—N8—C18	127.7 (2)	C25—C24—C11	126.6 (2)
C12—N8—C18	124.2 (2)	C29—C24—C11	111.9 (2)
C6—C1—C2	118.8 (3)	C26—C25—C24	119.9 (3)
C6—C1—C7	120.7 (3)	C26—C25—H25	120.1
C2—C1—C7	120.5 (3)	C24—C25—H25	120.1
C6—C1—Os	72.50 (16)	C25—C26—C27	120.9 (2)
C2—C1—Os	69.07 (16)	C25—C26—H26	119.6
C7—C1—Os	127.5 (2)	C27—C26—H26	119.6
C3—C2—C1	120.1 (3)	C26—C27—C28	118.3 (2)
C3—C2—Os	69.42 (16)	C26—C27—C30	120.9 (2)
C1—C2—Os	73.26 (16)	C28—C27—C30	120.8 (2)
C3—C2—H2	120.0	C27—C28—C29	122.9 (2)
C1—C2—H2	120.0	C27—C28—H28	118.5
Os—C2—H2	129.8	C29—C28—H28	118.5
C2—C3—C4	122.6 (3)	C28—C29—C24	116.5 (2)
C2—C3—Os	72.52 (17)	C28—C29—Os	125.9 (2)
C4—C3—Os	72.71 (17)	C24—C29—Os	117.53(19)
C2—C3—H3	118.7	C35—C30—C31	117.6 (3)
C4—C3—H3	118.7	C35—C30—C27	121.1 (3)
Os—C3—H3	128.5	C31—C30—C27	121.3 (3)
C5—C4—C3	115.7 (3)	C32—C31—C30	121.0 (3)
C5—C4—C8	121.2 (3)	C32—C31—H31	119.5
C3—C4—C8	123.0 (3)	C30—C31—H31	119.5
C5—C4—Os	69.80 (16)	C33—C32—C31	120.6 (3)
C3—C4—Os	68.89 (16)	C33—C32—H32	119.7
C8—C4—Os	131.3 (2)	C31—C32—H32	119.7
C4—C5—C6	123.0 (3)	C32—C33—C34	119.3 (3)
C4—C5—Os	72.22 (16)	C32—C33—H33	120.4

C6—C5—Os	75.02 (16)	C34—C33—H33	120.4
C4—C5—H5	118.5	C33—C34—C35	120.4 (3)
C6—C5—H5	118.5	C33—C34—H34	119.8
Os—C5—H5	126.2	C35—C34—H34	119.8
C1—C6—C5	119.5 (3)	C30—C35—C34	121.1 (3)
C1—C6—Os	70.85 (16)	C30—C35—H35	119.5
C5—C6—Os	67.52 (15)	C34—C35—H35	119.5
C1—C6—H6	120.2	O4—C36—O3	126.7 (3)
C5—C6—H6	120.2	O4—C36—C37	120.3 (3)
Os—C6—H6	134.9	O3—C36—C37	112.9 (3)
C1—C7—H7A	109.5	C36—C37—H37A	109.5
C1—C7—H7B	109.5	C36—C37—H37B	109.5
H7A—C7—H7B	109.5	H37A—C37—H37B	109.5
C1—C7—H7C	109.5	C36—C37—H37C	109.5
H7A—C7—H7C	109.5	H37A—C37—H37C	109.5
H7B—C7—H7C	109.5	H37B—C37—H37C	109.5
C10—C8—C4	113.6 (3)	C11—C38—C12	112.7 (6)
C10—C8—C9	108.7 (3)	C11—C38—H38A	109.0
C4—C8—C9	112.8 (3)	C12—C38—H38A	109.0
C10—C8—H8	107.1	C11—C38—H38B	109.0
C4—C8—H8	107.1	C12—C38—H38B	109.0
C9—C8—H8	107.1	H38A—C38—H38B	107.8
C8—C9—H9A	109.5	C40—C39—C44	120.0
C8—C9—H9B	109.5	C40—C39—C45	111.6 (10)
H9A—C9—H9B	109.5	C44—C39—C45	128.4 (10)
C8—C9—H9C	109.5	C39—C40—C41	120.0
H9A—C9—H9C	109.5	C39—C40—H40	120.0
H9B—C9—H9C	109.5	C41—C40—H40	120.0
C8—C10—H10A	109.5	C42—C41—C40	120.0
C8—C10—H10B	109.5	C42—C41—H41	120.0
H10A—C10—H10B	109.5	C40—C41—H41	120.0
C8—C10—H10C	109.5	C41—C42—C43	120.0
H10A—C10—H10C	109.5	C41—C42—H42	120.0
H10B—C10—H10C	109.5	C43—C42—H42	120.0
N5—C11—N8	110.9 (2)	C42—C43—C44	120.0

N5—C11—C24	116.2 (2)	C42—C43—H43	120.0
N8—C11—C24	132.9 (2)	C44—C43—H43	120.0
N8—C12—C13	131.6 (2)	C43—C44—C39	120.0
N8—C12—C17	106.7 (2)	C43—C44—H44	120.0
C13—C12—C17	121.7 (2)	C39—C44—H44	120.0
C14—C13—C12	117.0 (3)	C39—C45—H45A	109.5
C14—C13—H13	121.5	C39—C45—H45B	109.5
C12—C13—H13	121.5	H45A—C45—H45B	109.5
C13—C14—C15	121.4 (3)	C39—C45—H45C	109.5
C13—C14—H14	119.3	H45A—C45—H45C	109.5
C15—C14—H14	119.3	H45B—C45—H45C	109.5
C16—C15—C14	121.4 (3)		

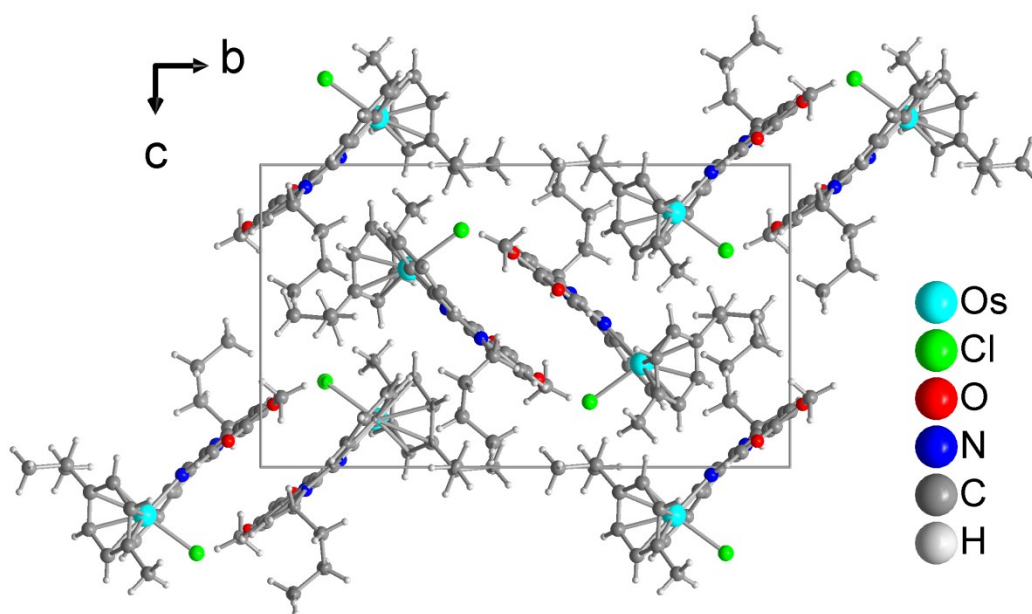


**Figure S29.** Packing diagram of complex 1.

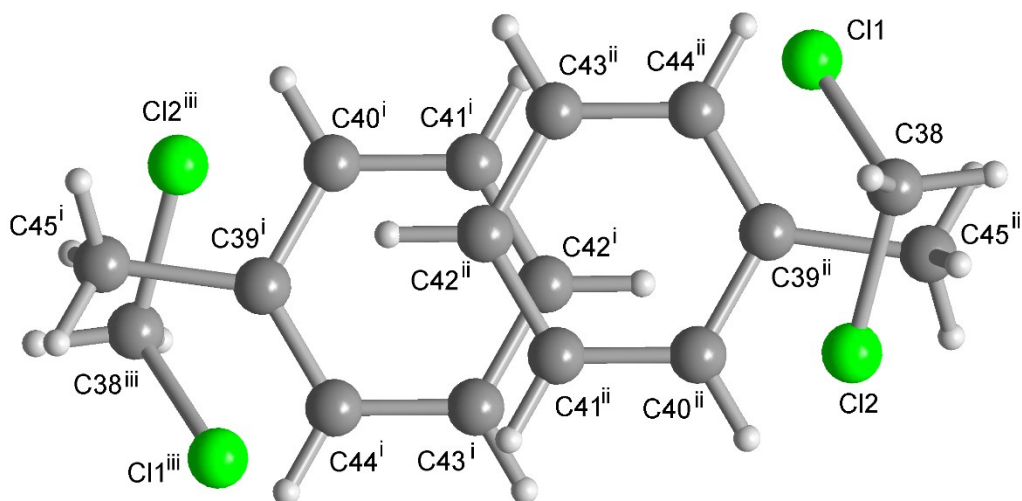


**Figure S30.** Assembly of the half-occupied  $\text{CH}_2\text{Cl}_2$  and toluene molecules around an inversion center in the crystal packing of **6**. Symmetry transformations:  $i = x, 1+y, z$ ;  $ii = 1-x, 1-y, -z$ ;  $iii = 1-x, 2-y, -z$ .

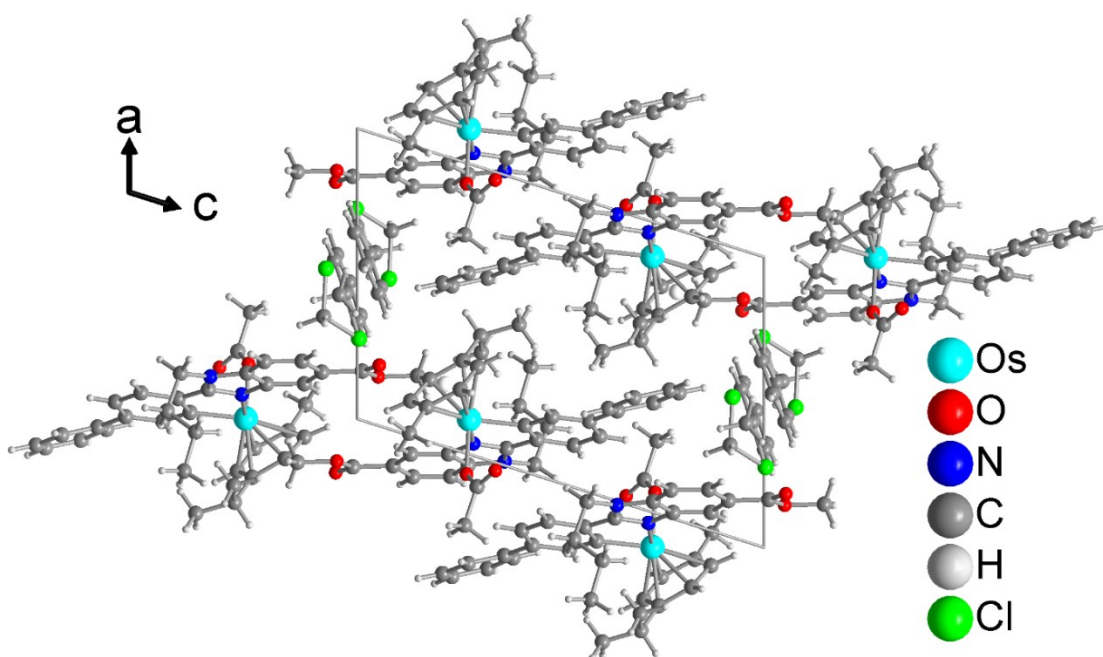
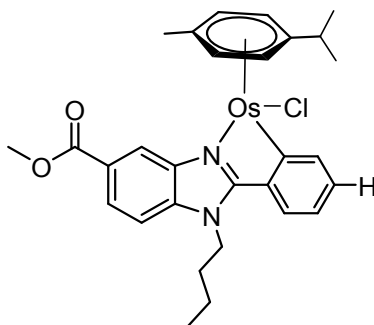


**Figure. S31.** Packing diagram of **6**.

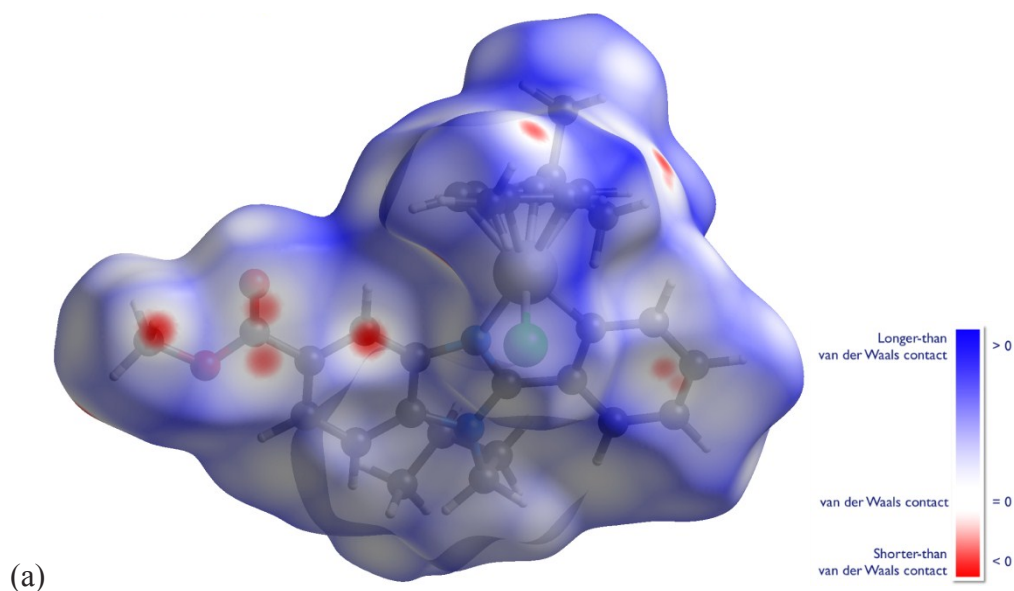
### *Supramolecular packing analysis for compound 1*

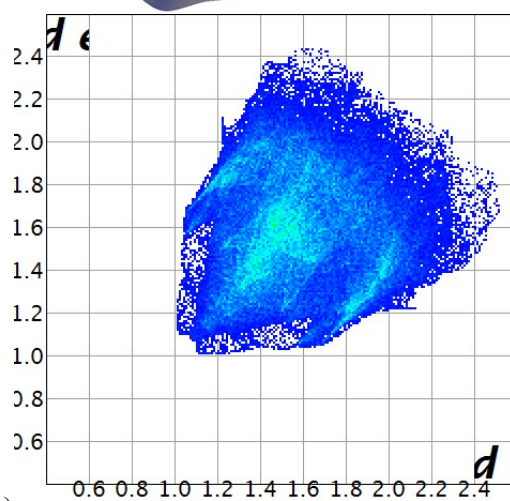
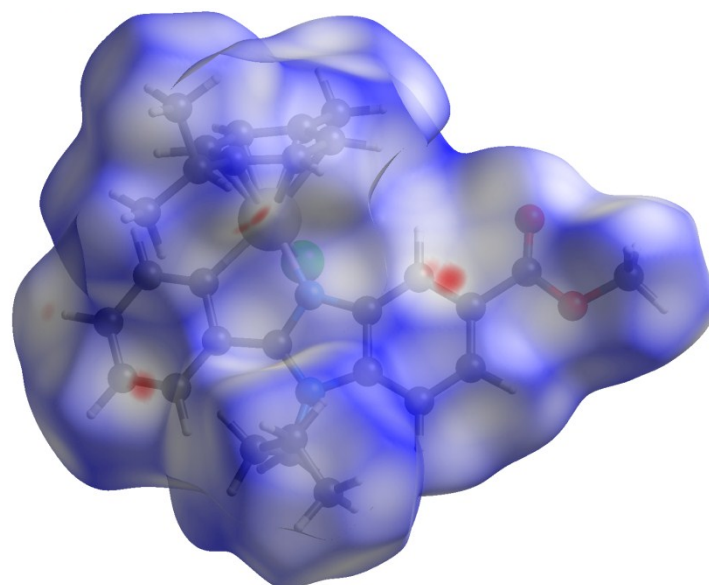
The supramolecular packing of compound **1** was analyzed in detail as an example for the supramolecular packing in this type of complexes. The results can be extended to the other complexes as well in view of their close structural similarity.

The supramolecular packing analyses in the solid-state structure of chlorido-(1-methyl-4-isopropyl-benzene)-(N-n-butyl-(phenyl)(methylester)benzimidazol- $\kappa^2$ N,C)osmium(II) (**1**) was carried out by a quantitative analysis of non-covalent intermolecular interactions with Hirshfeld surfaces using the program CrystalExplorer<sup>9</sup> following the methodology outlined in ref.<sup>10</sup>

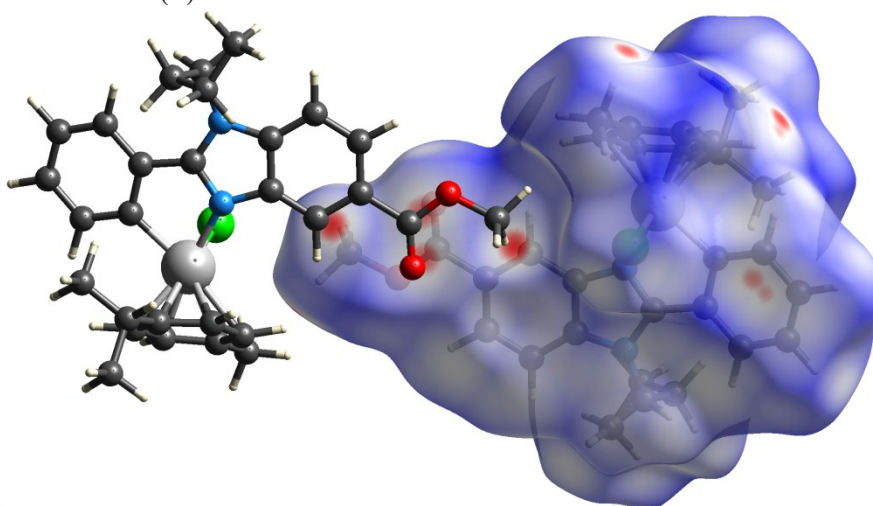


The Hirshfeld surface ( $d_{\text{norm}}$ ) of **1** displays close intermolecular contacts around the methyl ester and adjacent aryl ring and around the methyl and isopropyl group of the benzene ligand (red spots on the  $d_{\text{norm}}$  surface) (**Fig. S32**). The majority of the surface is colored blue (representing the sum of longer than van-der-Waals contact distances). The relative contributions to the Hirshfeld surface area due to close intermolecular contacts are summarized in **Table S8**. Noteworthy,  $\text{C}\cdots\text{C}$  (i.e.  $\pi\cdots\pi$ ) interactions are virtually non-existent.





(b)



(c)

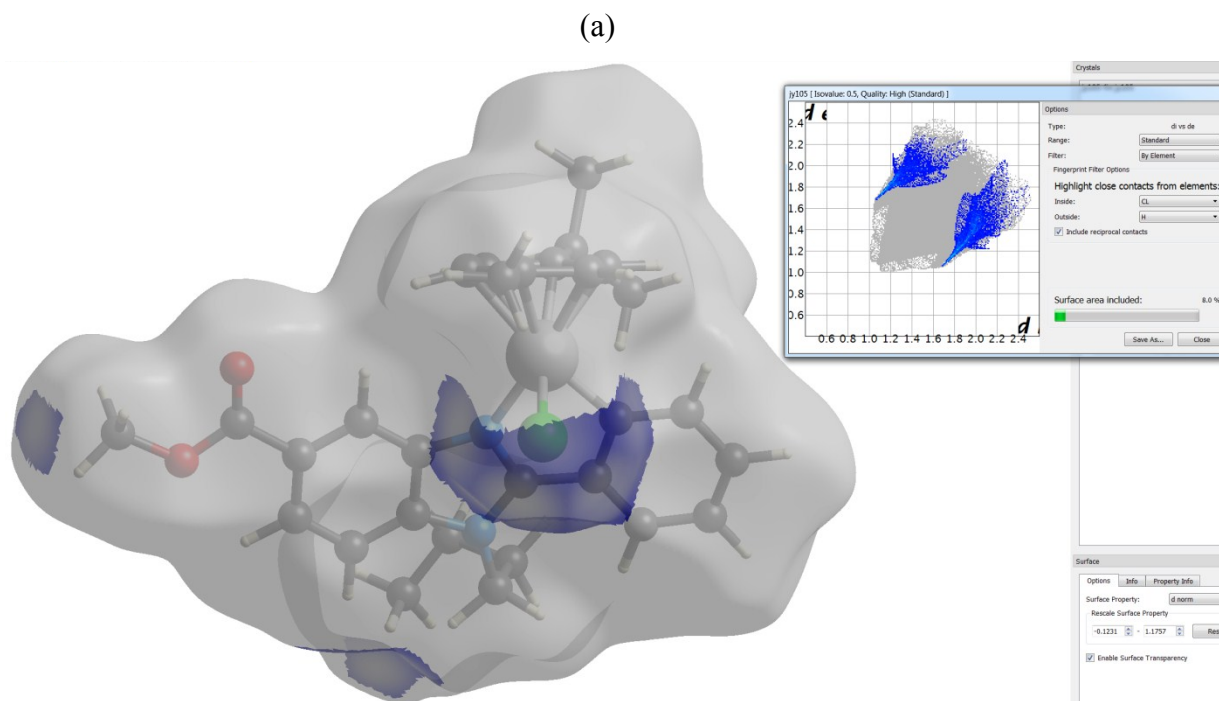
**Figure S32** (a) Hirshfeld surface of **1** mapped with the  $d_{\text{norm}}$  property – with two views from opposite side.<sup>10c</sup> Red represents the closest contacts, and blue the most distant contacts. (b) 2D fingerprint plot of **1**.  $d_i$  (abscissa) and  $d_e$  (ordinate) are the distances from

the surface to the nearest atom interior and exterior to the surface, respectively. For a breakdown of the fingerprint plot into the contributions from Cl $\cdots$ H, O $\cdots$ H, C $\cdots$ O, C $\cdots$ C, C $\cdots$ H and H $\cdots$ H close intermolecular contacts, see Table S8 and Fig. S33 and S34. (c) The interaction of the methyl ester moiety is a complementary C-H $\cdots$ C and C $\cdots$ O interaction of two inversion-symmetry related molecules (see also Fig. S34).

**Table S8.** Percent contributions of close supramolecular interactions to Hirshfeld surface in **1**.

Interaction	Percent (%)	Figure
Cl $\cdots$ H <sup>a</sup>	8.0	Fig. S33(a)
O $\cdots$ H <sup>a</sup>	7.2	Fig. S33(b)
C $\cdots$ O <sup>a</sup>	1.3	Fig. S34(a)
C $\cdots$ C (i.e. $\pi\cdots\pi$ )	0.3	no Figure
C $\cdots$ H (i.e. C-H $\cdots\pi$ ) <sup>a</sup>	19.7	Fig. S34(b)
H $\cdots$ H <sup>a</sup>	61.3	Fig. S34(c)
Sum	97.8	

<sup>a</sup> includes reciprocal contacts.



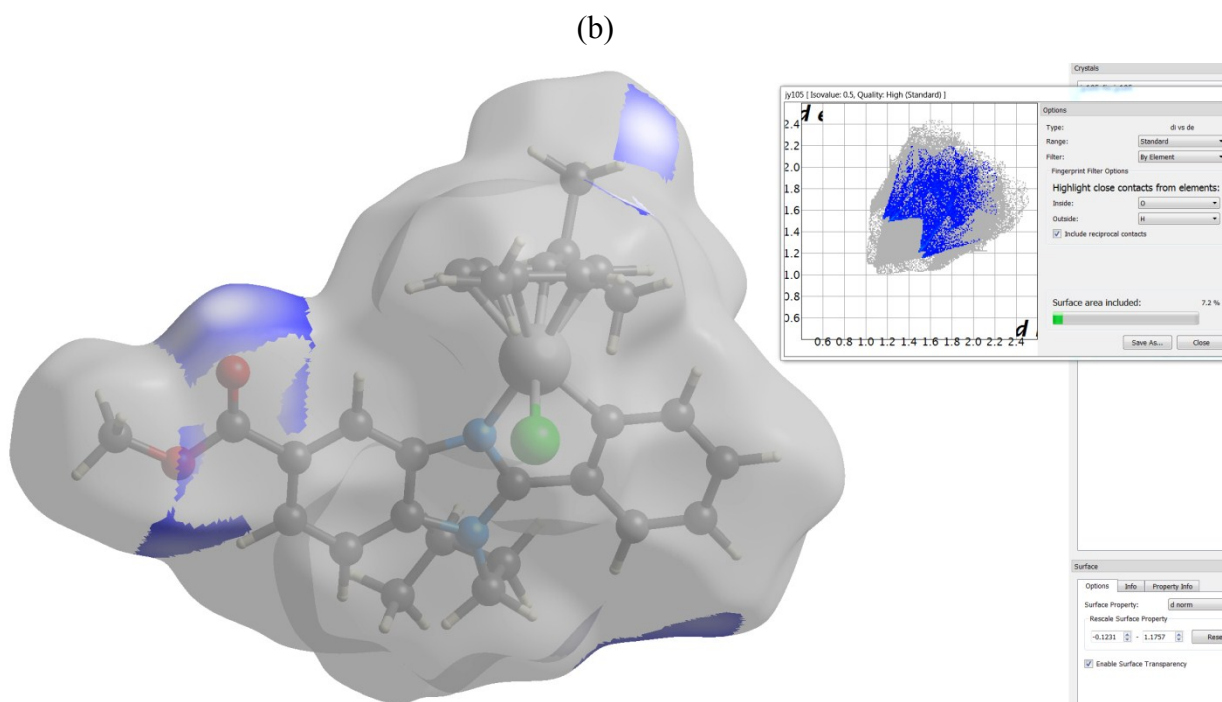
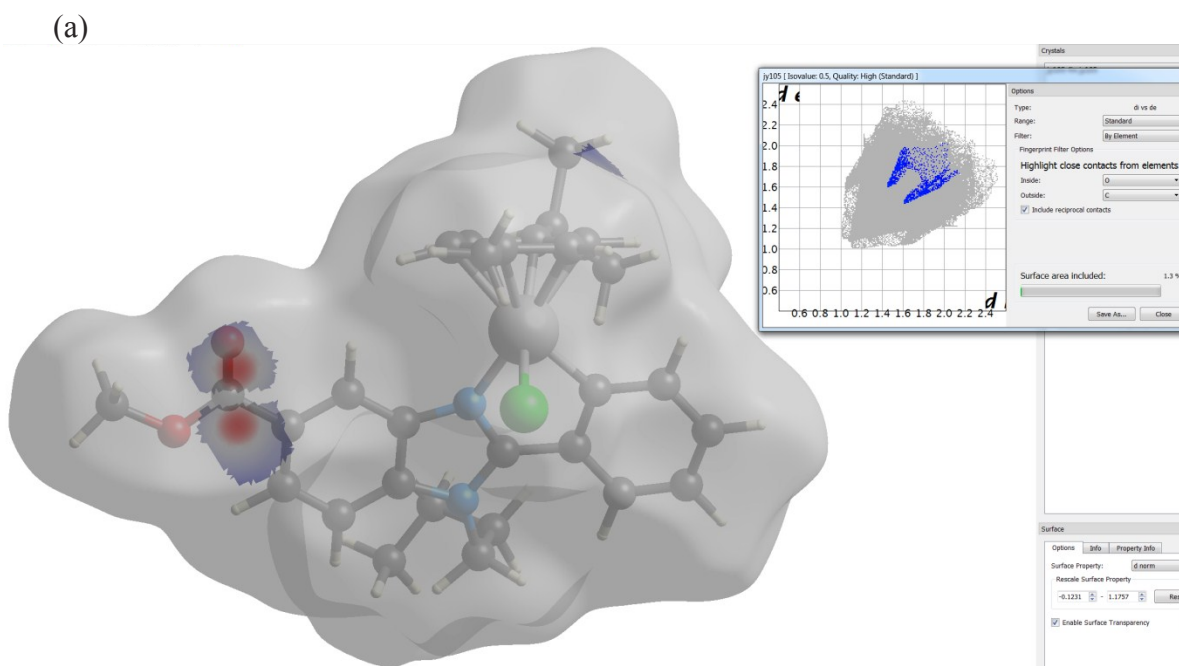


**Fig. S33** Relative contributions to the Hirshfeld surface area for the various close intermolecular contacts in **1** as graphical presentation of Hirshfeld surface with 2D fingerprint plot ( $d_i$  – abscissa and  $d_e$  – ordinate are the distances from the surface to the nearest atom interior and exterior to the surface, respectively).

(a) Cl $\cdots$ H.

(b) O $\cdots$ H.

Both 2D fingerprint plots show that these (C-)H $\cdots$ Cl and (C-)H $\cdots$ O contacts are not pronounced as two sharp features pointing to the lower left of the plot beyond the rest of the fingerprint plot as would be expected for strong H bonds (the upper area is the one corresponding to the H-bond donor, and the lower one to the acceptor).<sup>10b</sup>



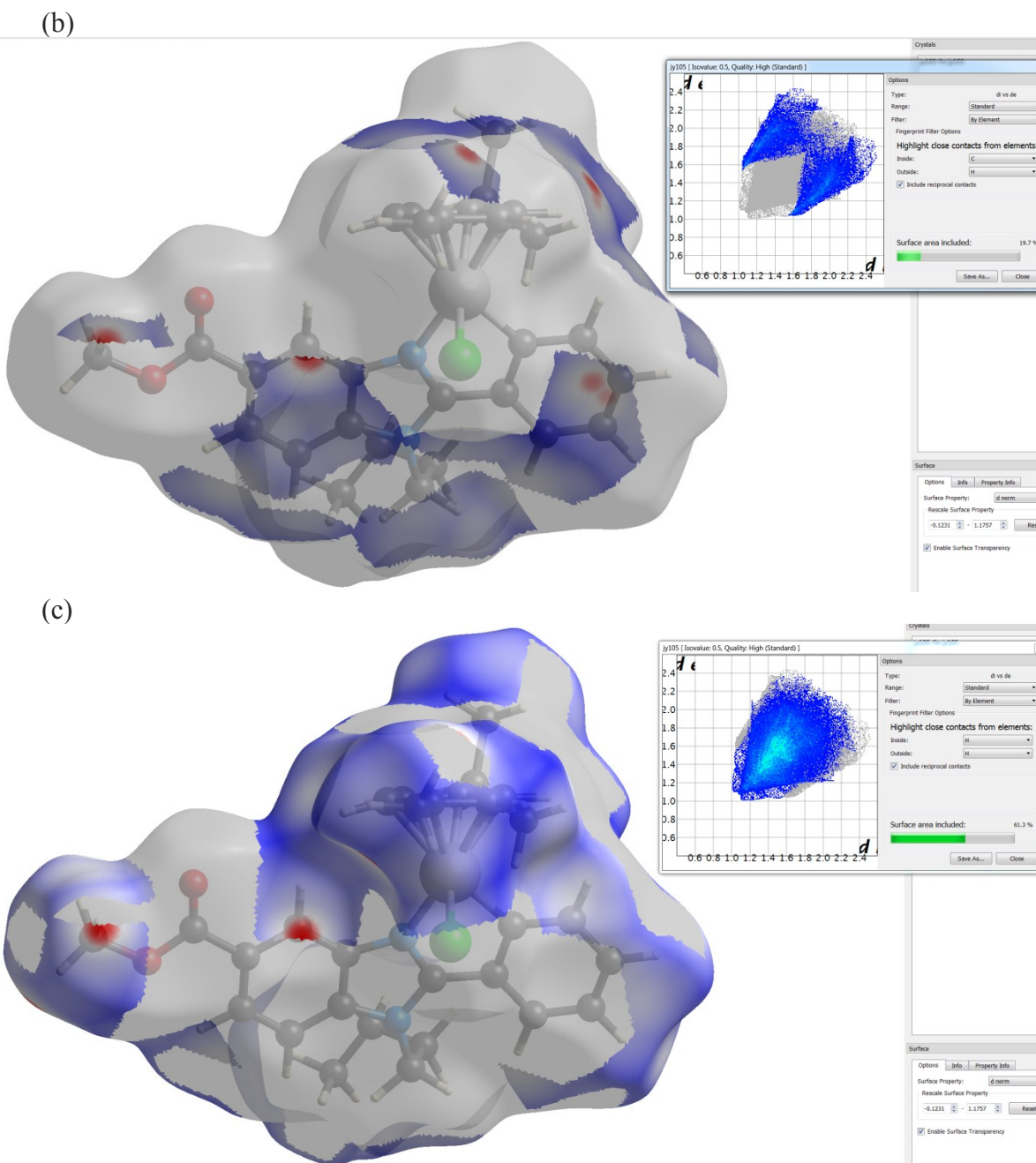


**Fig. S34** Relative contributions to the Hirshfeld surface area for the various close intermolecular contacts in **1** as graphical presentation of Hirshfeld surface with 2D fingerprint plot ( $d_i$  – abscissa and  $d_e$  – ordinate are the distances from the surface to the nearest atom interior and exterior to the surface, respectively).

(a)  $C \cdots O$ .

(b)  $C \cdots H$  (i.e.  $C-H \cdots \pi$ ). There are no very strong  $C-H \cdots \pi$  interactions, as ‘Wings’ at the upper left and lower right in the 2D fingerprint plot that are characteristic of strong  $C-H \cdots \pi$  interactions are absent.<sup>10b</sup>

(c)  $H \cdots H$ .

## References

- 
- <sup>1</sup> M. Brown, X. L. R. Fontaine, N. N. Greenwood, J. D. Kennedy *J. Organomet. Chem.*, 1987, **325**, 233-246.
- <sup>2</sup> G. S. Yellol, A. Donaire, J. G. Yellol, V. Vasylyeva, C. Janiak, and J. Ruiz, *Chem. Commun.*, 2013, **49**, 11533–11535.
- <sup>3</sup> J. G. Yellol, S. A. Pérez, A. Buceta, G. S. Yellol, A. Donaire, P. Szumlas, P. J. Bednarski, G. Makhloufi, C. Janiak, A. Espinosa and J. Ruiz, *J. Med. Chem.*, 2015, **58**, 7310-7327.
- <sup>4</sup> H. Zhang, L. Guo, Z. Tian, M., S. Zhang, Z. Xu *Chem. Commun.*, 2018, **54**, 4421-4424.
- <sup>5</sup> T. R. Chen, *TCA Manual*, 1975, **1**, 229–232
- <sup>6</sup> G. M. Sheldrick, *Acta Crystallogr. Sect. A* 2018, **64**, 112.
- <sup>7</sup> G.M. Sheldrick, Program SADABS, University of Göttingen, Göttingen, Germany (1996).
- <sup>8</sup> DIAMOND 4.4 for Windows. Copyright 1997-2017, Crystal Impact Gbr, Bonn, Germany; <http://www.crystalimpact.com/diamond>.
- <sup>9</sup> *CrystalExplorer17*, Version 17.5; Turner, M. J.; McKinnon, J. J.; Wolff, S. K.; Grimwood, D. J.; Spackman, P. R.; Jayatilaka, D.; Spackman, M. A. © 2005-217 University of Western Australia, 2017. <http://hirshfeldsurface.net>
- <sup>10</sup> (a) J. J. McKinnon, M. A. Spackman, A. S. Mitchell, *Acta Cryst.* 2004, **B60**, 627-668.  
(b) M. A. Spackman, J. J. McKinnon, *CrystEngComm*, 2002, **4**, 378–392.  
(c) J. J. McKinnon, D. Jayatilaka, M. A. Spackman, *Chem. Commun.*, 2007, 3814–3816.